Title

A fully synthetic route towards simplified pleuromutilin antibiotic candidates

Author

Tran, Arthur Alexandre

Publication Date

2024

Peer reviewed|Thesis/dissertation

A fully synthetic route towards simplified pleuromutilin antibiotic candidates

by
Arthur Alexandre Tran

DISSERTATION
Submitted in partial satisfaction of the requirements for degree of
DOCTOR OF PHILOSOPHY

in

Chemistry and Chemical Biology

in the

GRADUATE DIVISION
of the
UNIVERSITY OF CALIFORNIA, SAN FRANCISCO

Approved:

Signed by:
Ian Seiple
0F55EF21BB3D419...

Ian Seiple
Chair

Signed by:
William DeGrado
DocuSigned by:
Adam Renslo
FBDB6299FCD244B...

William DeGrado

Adam Renslo

Committee Members

This thesis is dedicated to my parents, who were the ones that provided me the opportunity to pursue higher education. I wouldn't have made it here without your love and support.

“I love deadlines. I love the whooshing noise they make as they go by.”

- Douglas Adams

Acknowledgements

Where do I even begin? To say that graduate school was a tumultuous time would be a severe understatement, and I have so many people to thank for supporting me every step of the way.

I want to thank my parents, Christopher and Sylvie, to whom this work is dedicated. Their unconditional love and support for my life pursuits have made it possible for me to get this far in my education, and I am forever grateful of the sacrifices they've made to ensure a good life for me and my sister. Thank you for all the meal prepped food that you've dropped off for me and for all the times you would take me out for lunch at my one of my favorite Chinese restaurants in Millbrae. I also want to thank my grandfather, Bernard Tran. I'm sorry I couldn't finish sooner so you could see me walk. Thank you for all the calls reminding me to take care of myself and rest.

I want to thank my PhD advisor, Dr. Ian Seiple, for being an absolutely amazing boss and mentor. In 2016, when I was still an undergraduate student at UC Berkeley, I struggled to find a research position in the College of Chemistry. Thank you for being the first person to give me a chance to do research. I never would have thought that I would be working for you for the next 8 years, but I'm glad that I was able to see your lab at UCSF from beginning to end. I'll never forget the Christmas card you gave me encouraging me to apply to graduate school. Thank you for the rigorous training in chemistry and life lessons along the way.

To the rest of the Seiple lab, I want to thank nearly all the members who have come through. From the beginning, I'd like to thank Dr. Qi Li, Dr. Yanmin Yao, and Dr. Lingchao Cai for their chemistry guidance and teaching me lab technique that I still use to this very day. Thank you, Ruoxi and David, for being my fellow undergraduate students from Berkeley and making the early days of the lab less intimidating. Thank you, Charly, for bringing life to the lab for the first summer I was there and really jumpstarting the positive lab culture we have now. Thank you, Dr. Yoshito Takahashi, for being an incredible postdoc mentor and cheering me on whenever science got difficult. Thank you to Dr. Seul Ki Yeon, for being an amazing coworker and one that I want to be like as I move onto becoming a postdoc myself. Thank you, Dr. Minh Tran, for being a reliable friend and colleague, whether it was discussing science and life, going to the gym, or grabbing boba in the afternoons. Thank you, Quinn Edmondson, for being one of the closest friends I've made in graduate school. I would say I'm going to miss the inside jokes, the ridiculous work shenanigans, and the many laughs we've had over the years, but I'm glad to say that we'll get to continue our antics in our postdoc as we move onto the same lab. Thank you, Andrew Ecker, for being one of the most intelligent and thoughtful graduate students to have come through our lab, and for all the discussions about reaction conditions and NMR experiments. Thank you, Isabel Lee, Leo Chen, and Jesus Madrigal for being a few of the best lab mates a scientist could ask for.

To the broader UCSF community, I want to thank other friends I've made along the way: Dr. Katarina Pance, Dr. Lawrence Zhu, Dr. Letitia Sarah, and Dr. Evelyn Strickland. Grad school has been a tough ride, but it was made infinitely better getting to know all of you. To my partner in our collaboration with the Wells lab, thank you to Dr. Sophie Kong for teaching me the skills I need to be a chemical biologist. I also want to thank the numerous mentors I've had the fortune to meet:

Dr. Douglas Wassarman, Dr. Kaitlyn Tsai, Dr. Shizhong Dai, Dr. Kangway Chuang, Dr. Huong Kratochvil, and of course Dr. Ziyang Zhang. Thank you for all of the advice you've all provided throughout my years as a graduate student. I would also like to extend my thanks to my thesis committee members Dr. William DeGrado and Dr. Adam Renslo for their scientific insight and guidance in my projects.

To my friends outside of science, I want to thank my friends from home back in Milpitas, John Leung and Eric Hua. Thank you for going out of your way to come and see me in San Francisco when I was at my lowest and for giving me people to look forward to seeing whenever I did go home. To my sister Melody and her partner Andy, thank you for spending time with me when I needed it most and for bringing along Koda and Artemis to keep me company. To my old roommates and still close friends to this day, thank you Chloe Li for all the fun trips and adventures we've had since living together in college, and thank you Kristen Shimoda for all the music recommendations that make up the backbone of my playlists. To Alyssa Yu, thank you for being the best friend from hundreds of miles away and for all the hour-long phone calls we've had catching up with one another.

Thank you, Patrick and Sora, for being there for me for nearly the entirety of graduate school. I know for certain that I wouldn't have made it this far in one piece without your constant care and support, and for that, I am eternally grateful.

Contributions

The chapters in this dissertation were performed under the guidance of Dr. Ian B. Seiple, with the collaboration and feedback of many other Seiple lab members. My thesis committee members, Dr. William DeGrado and Dr. Adam Renslo, also provided important scientific guidance that were important in pushing these projects forward.

Chapter 1: Unpublished work that has not yet been submitted for publication. This chapter contains the majority of my thesis work, which is on developing a platform for synthesizing simplified pleuromutilin antibiotic candidates. Arthur Tran conceptualized the synthetic route and performed the synthesis of compounds. Arka Rao and Sungwon Jung performed the synthesis of intermediates in the route.

Chapter 2: Unpublished work that has not yet been submitted for publication. This chapter details the development of antibody-drug conjugates for the targeted degradation of G-protein coupled receptors. Katarina Pance and James A. Wells conceptualized the project. Sophie Kong conceptualized and performed degradation experiments. Arthur Tran performed the synthesis of compounds, bioconjugation, and degradation experiments.

Arthur Tran provided the much of the manuscript preparation of this dissertation, which is a substantive contribution comparable to other dissertations in Chemistry & Chemical Biology. Ian B. Seiple directed and supervised the research and provided guidance and feedback throughout.

A fully synthetic route towards simplified pleuromutilin antibiotic candidates

Arthur Alexandre Tran

Abstract

(+)-Pleuromutilin is a fungal natural product that binds to the peptidyl transferase center of bacterial ribosomes, inhibiting protein synthesis as its mechanism of action. This tricyclic diterpene has been successfully modified through semi-synthesis to access more potent analogs such as the recently FDA-approved lefamulin, which is used for treating adults with community – acquired bacterial pneumonia. However, semi-synthesis provides an inherently restricted approach to incorporating variations in the structure of chemical matter. Thus, pleuromutilins remain limited in their spectrum of activity and susceptible to modifications in the ribosomal binding site that confer resistance. Previous studies have provided evidence that modifications of the core are well-tolerated in that fully synthetic analogs may retain biological activity. Here, we will describe our efforts in developing an efficient synthesis of pleuromutilin that may not strictly follow its natural substitution pattern, but will allow for the construction of a diverse library of simplified pleuromutilin analogs.

In Chapter 1, we report a synthetic route towards simplified pleuromutilin antibiotic candidates that uses a key photochemical reaction to access the six-, eight-membered bridged ring system. We describe our efforts in optimizing steps in this route, including the conditions necessary for the [2+2] cycloaddition in the de Mayo-type reaction sequence.

In Chapter 2, we report the synthesis of antibody-drug conjugates for the targeted degradation of cell surface proteins.

Table of Contents

List of Figures

Chapter 1

A photochemical approach towards bridged bicycle analogs of pleuromutilin

Abstract

We are at the precipice of entering a post-antibiotic era. There is an urgent need for novel antibiotics, and revisiting previously discovered classes with modern synthetic techniques may revitalize their development. Pleuromutilin is one such known antibiotic that has been heavily underexploited for human use due to the limitations placed on medicinal chemistry by the molecule's complex scaffold and lack of functional handles. From previous syntheses and studies of this class of antibiotics, it has been found that certain modifications of the core scaffold, such as removing methyl groups, are well-tolerated and do not necessarily ablate biological activity. Most notably, cleavage of one of the rings in the tricyclic core provides pleuromutilin analogs that are still active, suggesting that natural product simplification can lead to a novel carbocyclic scaffold with potential as a versatile medicinal chemistry fragment. In this work, we describe a synthetic approach that accesses the 6,8-bridged ring system of pleuromutilin through a key de-Mayo type reaction sequence. This strategy enables the synthesis of a library of simplified bridged bicyclic analogs, which will be used to explore structural determinants of antibacterial activity and identify novel antibiotic candidates.

Introduction

The rise of antibiotic resistance is a global concern that threatens to undo significant advances in human medicine. The continued overuse of antibiotics in the clinic and for livestock has led to the emergence of multidrug-resistant bacteria, resulting in the increasing need to turn to "last resort" treatments.[1] Coupled with the fact that the pharmaceutical industry has moved away from investing in antibiotic development, we are at risk of running out of efficacious drugs against pathogenic bacteria.[2] Entering a post-antibiotic era could cause common bacterial infections, and even routine surgical procedures, to become life-threatening. Thus, there is a clear and urgent need for the development of novel antimicrobials.

The ribosome is one of the most prolific targets in the bacterial cells for antibiotics, as protein synthesis is necessary for cell viability.[3] The prokaryotic ribosome (70S) consists of the large 50S subunit and the small 30S subunit, and antibiotics can bind to select sites on the complex to inhibit translation. The peptidyl transferase center (PTC), located on the 50s subunit, is one such location where antibiotics can bind to inhibit peptide-bond formation by disrupting the positioning of the aminoacylated ends of tRNAs.[4] Clinically important antibiotic classes that bind to the ribosome at this site include pleuromutilins, chloramphenicols, lincosamides, streptogramins, and oxazolidinones (**Figure 1.1**).[5]

Pleuromutilins are a class of antibiotics that consist of the natural product pleuromutilin (**1)** and its semisynthetic derivatives **2-6** (**Figure 1.2**).[6] Discovered by Kavanagh and coworkers in 1951 from cultures of the fungi *Pleurotus mutulis* (known as *Cliopilus scyphoides*) and *Pleurotus passeckeranius*, pleuromutilin was found to have modest activity against in Gram-positive cocci

(MIC = 0.25 μg/mL in *Staphylcoccus aureus*) and some activity against fastidious Gram-negatives (eg. *Haemophilius influenza*).[7-9] Further studies revealed that the compound was active against penicillin and streptomycin-resistant staphylococci as well as *Mycoplasma* spp, prompting the pharmaceutical industry to initiate pleuromutilin research programs.[10,11] Early semisynthetic work on the molecule led to the development of tiamulin (1979, Sandoz Pharmaceuticals) and valnemulin (1999, Novartis), two veterinary antibiotics available for oral and intramuscular delivery.[6, 12,13]

Despite their extensive use in veterinary medicine over the past couple of decades, pleuromutilin antibiotics are comparatively underdeveloped for use in humans. While oral valnemulin has been reported to be effective in treating immuno-compromised patients with resistant mycoplasma infections, the first pleuromutilin antibiotic for human use was not approved until 2007 with the introduction of retapamulin (GlaxoSmithKline).[14,15] However, retapamulin is not available in systemic dosage form and remains a topical agent for short-term treatment of infected small lacerations and impetigo. This highlights a central challenge in developing pleuromutilin antibiotics for human use: they have a propensity to be metabolically unstable.[16] For example, azamulin (**6**) is an azole derivative of pleuromutilin that was developed for human use, but was found to be rapidly metabolized by cytochrome P450 oxidation and excreted.[17] The poor pharmacokinetics of pleuromutilin derivatives were believed to be a standing issue with the class, and it was not until recently that these shortcomings were overcome. Lefamulin (Nabriva Therapeutics) is an orally and intravenously available derivative that was approved in 2019 making it the first pleuromutilin antibiotic for systemic human use.[18] Despite significant improvements in metabolic stability, lefamulin still requires twice-daily dosing over a period of five to seven days.

Additionally, due to its limited spectrum of activity, it has only been indicated for the treatment of community-acquired bacterial pneumonia (CABP).

Pleuromutilin is a diterpene that contains a tricyclic carbon skeleton (made up of a five-, six-, and eight-membered ring system), eight stereocenters, and a glycolic ester functionality at the C14 position. The most extensively modified site of the molecule is the C14 glycolic ester side chain.[19] Modifications of this site typically either replace the entire chain with an acyl carbamate or replace the terminal hydroxyl group with a sulfanyl acetate, although the most successful derivatives thus far for the clinic are those containing the sulfanyl acetate functionality.[6,20] While it has been shown that modifications of the C14 side chain can result in improved PK/PD properties and contribute to lower minimal inhibitory concentrations (MICs), they are not known to expand the spectrum of activity nor address known resistance mechanisms of the pleuromutilin class.[21,22] As it stands, the C14 side chain remains the most investigated site of the molecule due to the presence of a reactive handle, whereas the mutilin core remains challenging to modify by semisynthetic means.

The synthesis of pleuromutilin has been pursued by the synthetic community, resulting in reports on various approaches to its unique scaffold as well as seven total syntheses.[23-30] However, due to the moderate linearity of these established routes, they are not conducive towards the synthesis of a diverse library of analogs for structural exploration. In one recently reported total synthesis, Herzon and coworkers designed a route that allowed access to not only pleuromutilin, but also its epimers at two carbon centers on the eight-membered ring.[26,27] Additionally, they were able to adapt this route to synthesize analogs with ring contractions about the five and eight-membered rings and other appendage modifications to the quaternary center of the eight-membered ring.[31] Of

the analogs reported, however, changes to ring size were detrimental to activity, whereas removal of a methyl on the quaternary center was well tolerated. Besides these analogs, very few core modifications to pleuromutilin have been reported.

A notable modification of the core is epimerization of the C12 center reported by Berner and coworkers (**Figure 1.3**). Upon treatment with ethyl zinc iodide and heating, pleuromutilin 22-O-tosylate **7** was found to undergo a retroallylation-allylation reaction at C12, producing a nearly equimolar mixture of the starting material and C12 epimer **8**.[32] This modification has been further studied by Nabriva Therapeutics, who have taken these 12-*epi*-pleuromutilins and functionalized the alkene with amine linkers. Intriguingly, this modification resulted in analogs with increased activity against a strain of *E. coli*.[33] In a follow-up study, Nabriva also found that 12-*epi*-pleuromutilins with an amine functionalized linker containing six to eight carbons also had an increased spectrum of activity against Gram-negative pathogens, including *Klebsiella pneumoniae*, *Citrobacter freundii*, and *Enterobacter cloacae*.[34] While the structures were not disclosed, these findings show that the C12 epimer is an ideal product that can provide potent pleuromutilin analogs through medicinal chemistry.

Another modification of interest to the mutilin core is the structural simplification reported by Sorensen and coworkers (**Figure 1.4a**).[35,36] The MICs of these simplified derivatives were determined for a strain of *M. tuberculosis*, revealing that these analogs still retained antimicrobial activity. This finding suggests that core modifications to pleuromutilin, such as removing methyl substituents, are tolerated.

Finally, in another study that exemplifies the promising activity of structurally simplified pleuromutilins, Springer and coworkers reported that cyclopentanone-cleaved derivatives were found to be active against *S. pneumoniae* and *S. aureus* (**Figure 1.4B**).[37] This is one of the very few reports of major modification to the ring structure in the tricyclic pleuromutilin core.

The aforementioned findings suggest that 1) core modifications, such as removing methyl substituents, are well tolerated and 2) the bicyclic system containing the six- and eight-membered rings (named a cis-bicyclo[5,3,1]undecane system) of pleuromutilin is sufficient for antibacterial activity and may provide a novel carbocyclic scaffold that could be generally useful as a medicinal chemistry fragment. Here, we report a synthetic strategy towards pleuromutilin antibiotics that is guided by these principles: our targets will contain the cis-bicyclo[5,3,1]undecane system with a secondary alcohol, quaternary center, and glycolic ester on the eight membered ring. Accessing this bicyclic system would allow for structural exploration of a potentially active minimized pharmacophore of pleuromutilin.

There have been sparse reports of the synthesis of the bicyclo[5,3,1]undecane system, as eight-membered rings are notoriously difficult to form. Reported methods include Grob fragmentation of a tricyclic undecane derivative and oxy-cope rearrangements of specifically prepared substrates, which are strategies that are not conducive to generating a library of analogs.[38-40] One of the most efficient syntheses of this bicyclic system utilized the de Mayo reaction, a photochemical reaction in which the enol of a 1,3-diketone (or β-keto ester) undergoes a [2+2] cycloaddition with an alkene to form a cyclobutane ring that is then cleaved through a retro-aldol reaction.[41] Inspired by previous work done by the Winkler group utilizing the de Mayo reaction sequence towards daphnane and ingenane diterpenes, we developed a synthetic strategy to access the bicyclo[5,3,1]undecane

system found in pleuromutilin (**Figure 1.5**).[42,43] A dioxenone photoreaction precursor can be synthesized in just 4 steps from an enone and alkene tether. Under the appropriate photochemical conditions, the alkene will undergo a [2+2] cycloaddition with the dioxenone to give a tetracyclic photoadduct. This intermediate can then undergo acetonide cleavage under basic conditions to give the desired bicyclic system.

Results

The current developed route toward simplified pleuromutilin analogs is outlined in **Figure 1.6**. Synthesis of the enone fragment commences with a nitrosobenzylation of commercially available **11** with catalytic L-proline, followed by Luche reduction of the ketone in the same pot. Palladium on carbon mediated hydrogenation of the nitrosobenzene functionality provided diol 1**3** in 66% yield over 3 steps. Ketal deprotection and concomitant elimination occurred under refluxing conditions with Amberlyst 15 to form enone **14**. in 71% yield. As this enone is prone to aromatization, it was immediately protected with a tert-butyldiphenylsilyl silyl group to afford intermediate **15**. Treatment with lithium diisopropylamide (LDA), followed by the addition of hexamethylphosphoramide (HMPA) and methyl iodide in succession, yielded monomethylated intermediate **16** as a 1.5:1 mixture of inseparable diastereomers in 86% yield. Conditions were explored in installing a vinyl group as part of the quaternary center (ie. an aldol reaction with (phenylseleno)acetaldehyde, followed by elimination in the presence of methanesulfonyl chloride), however, we opted to replace the vinyl group with another methyl group to simplify the sequence going into the key [2+2] cycloaddition. Again, treating monomethylated enone **16** with LDA, followed by addition of methyl iodide, afforded dimethylated enone **17** in 74% yield. Conjugate addition with 5-bromo-1-pentene through organocuprate formation yielded alkene **18**

as a 5:1 mixture of inseparable diastereomers in 86% yield, which could be separated after dioxenone formation.

With alkene **18** in hand, we looked to form the prerequisite dioxenone for the key photochemical reaction. We found that we could form a beta-keto ester with LDA and Mander's reagent, then form the dioxenone under acidic conditions in the presence of acetone.[44] However, the yield of the dioxenone formation step was poor (0-25% yield) and acted as a bottleneck in our synthetic route. Upon further optimization of the sequence, we found that we could instead treat alkene **18** with LDA and anisyl cyanoformate, and then treat the resultant para-methoxybenzyl beta-keto ester **19** with trifluoroacetic acid, trifluoroacetic anhydride, and acetone to obtain single product dioxenone **20** in a reproducible 27% yield (**Figure 1.7**).[45,46]

Now with a sequence that could reliably provide dioxenone **20** in modest yield, we took to screening photochemical conditions for the [2+2] cycloaddition (**Figure 1.8**). Initially, we found that the reported conditions by Winkler and co. to show total conversion of the dioxenone into photoadduct **21** after 2 hours of exposure to a 450W Hanovia Mercury lamp. 1H NMR revealed the loss of peaks corresponding to those of the protons on the alkene and could be used to monitor the reaction progression. We looked to see if milder conditions, such as using visible light, with the appropriate photosensitizer would also yield formation of the same photoadduct. However, thorough screening for the use of other solvents (eg. DCM, toluene, DMF) and other photosensitizers (eg. acetophenone, iridium-based catalysts) proved to be unfruitful. With regards to entry 6, we especially focused on using this reported catalyst in combination with 395 nm light, as it the original system described worked with beta-keto esters and alkenes.[47] If these conditions

could be applied to our key step, we could avoid forming a dioxenone altogether and skip one step in our route. However, the reported conditions did not work for our system, possibly due to a higher energy barrier to reaction in our intramolecular cyclization from additional ring strain. Nevertheless, we were able to find conditions that allowed us to move forward in our synthetic route with broad band UV light and acetone as a photosensitizer. At this stage in the synthesis, we also found the use of deuterated benzene would resolve peaks in 1H NMR quite clearly, especially between the 2-4 ppm region. With this in mind, we could clearly identify that there were actually two photoadducts formed, presumably products that depended on the face of approach of the alkene to the dioxenone. It has been noted previously that photochemical reactions with similar systems would also result in more than one product, although in our system specifically, cleavage of the acetonide would result in both photoadducts converging to the same six-, eight- membered bridged bicycle intermediates.[48]

With the key photochemical reaction complete, treatment of photoadduct **21** in a methanolic potassium hydroxide solution (2M KOH in MeOH) afforded the six-, eight- membered bridged bicyclic system as a mixture of diastereomers about the carboxylic acid (**Figure 1.9**). As the diastereomers were difficult to separate from one another, we opted to carry the material forward and resolve the mixture at a later stage. Methyl ester formation with TMS-diazomethane, followed by reduction of the ketone with sodium borohydride yielded alcohol **24**, which could be isolated and confirmed by 2D NMR (COSY and NOESY) to be the depicted diastereomer. Unfortunately, while the reduction appeared highly diastereoselective, the stereoisomer isolated does not have the same stereocenter about the alcohol on the eight-membered ring as pleuromutilin. However, as shown in previous studies on fully synthetic pleuromutilins, the stereocenter about this alcohol

could be inverted, and analogs would still retain biological activity.[36] In addition, we are currently exploring alternative reduction conditions to alter the stereoselectivity to bias the opposite direction.

Further studies are currently in progress to elaborate alcohol **24** into analogs for an initial set of bicyclic pleuromutilin analogs. Deprotection of the silyl group followed by esterification off of the newly revealed alcohol can provide simplified versions of pleuromutilin and Lefamulin, depending on the ester appended. The activity of synthesized pleuromutilin derivatives will be tested by minimum inhibitory concentration (MIC) assays against *S. aureus* and *E. coli*.

Figures

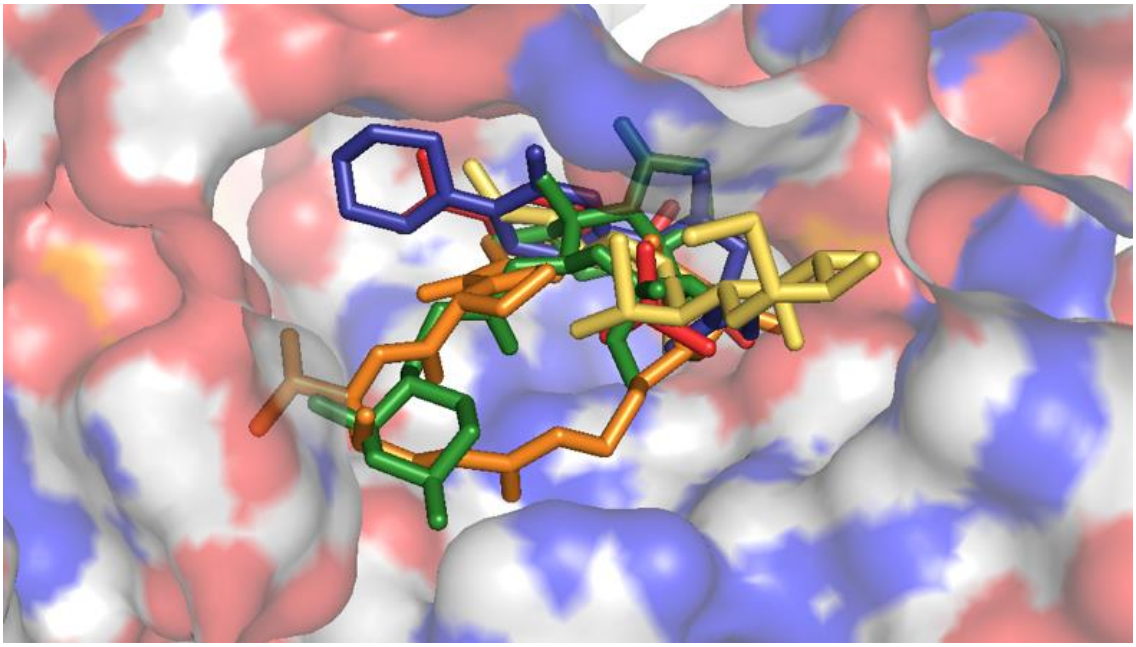

Figure 1.1: Antibiotics bound to the peptidyltransferase center (PTC) of the bacterial ribosome. (Streptogramin A: orange, pleuromutilin: green, lincosamide: yellow, oxazolidinone: red, phenicol: red)

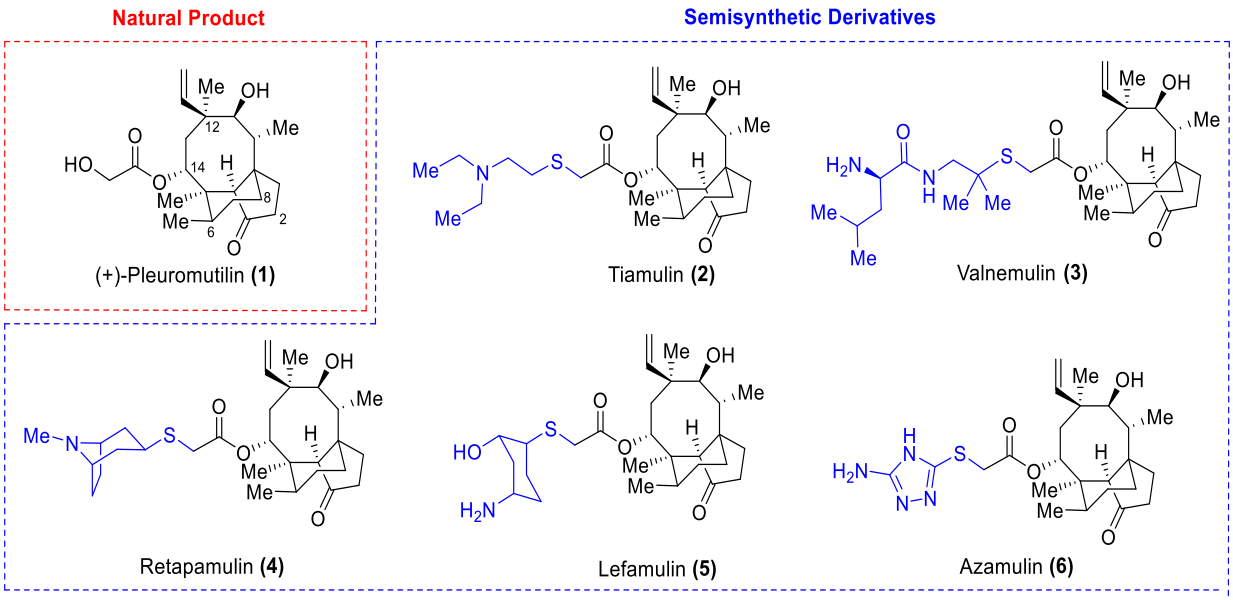

Figure 1.2: Selected pleuromutilin antibiotics with modifications highlighted.

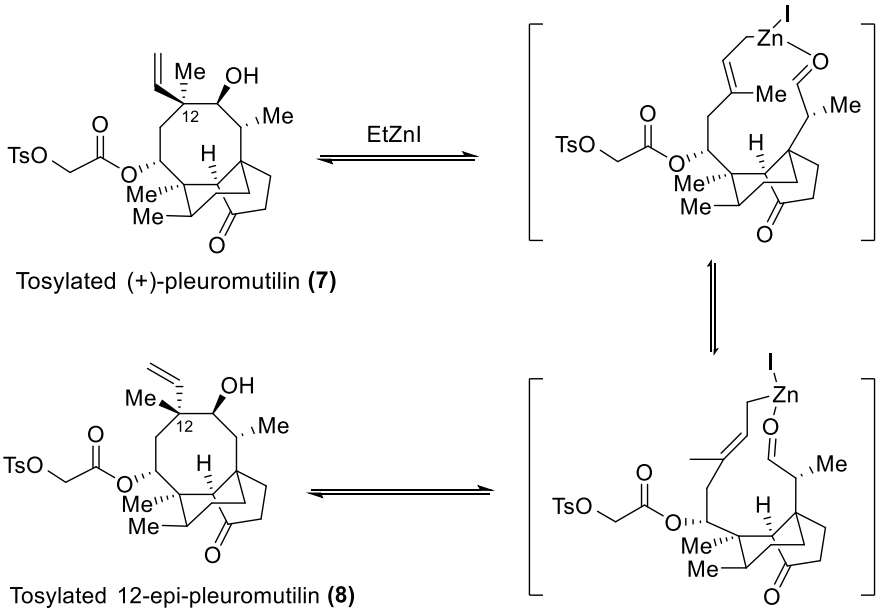

Figure 1.3: Epimerization of C12 mediated by ethyl zinc iodide.

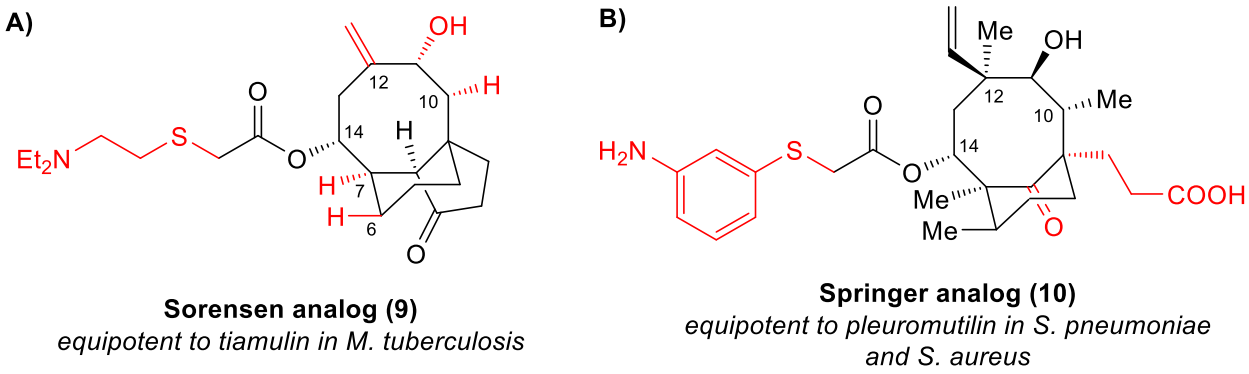

Sorensen analog (9)
equipotent to tiamulin in M. tuberculosis

Springer analog (10)
equipotent to pleuromutilin in S. pneumoniae and S. aureus

Figure 1.4: Examples of structurally simplified pleuromutilins. A. A structurally simplified analog of pleuromutilin was found by Sorenson and co. to be equipotent to tiamulin in *M. tuberculosis*. **B.** Cyclopentanone cleaved pleuromutilin was found by Springer and co. to be equipotent to pleuromutilin in *S. pneumoniae* and *S. aureus*.

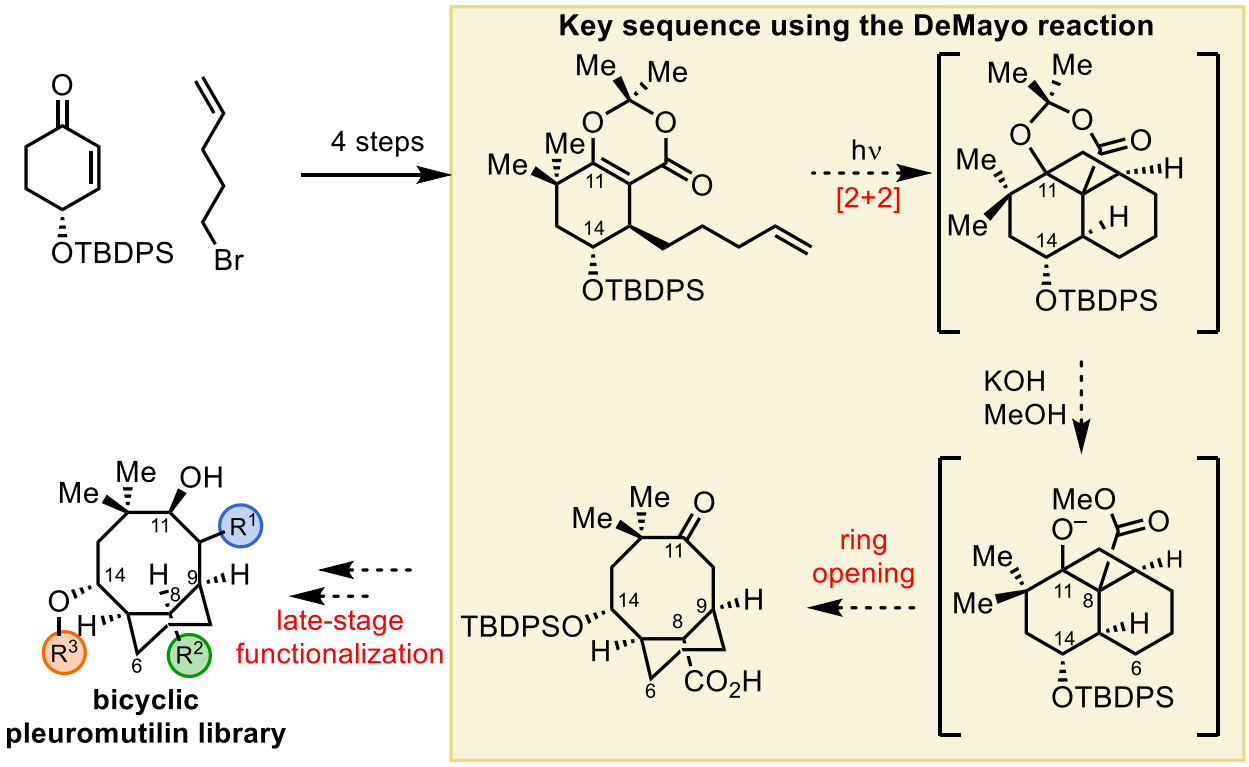

Figure 1.5: Key synthetic strategy towards analogs with a 6,8-bridged bicyclic system.

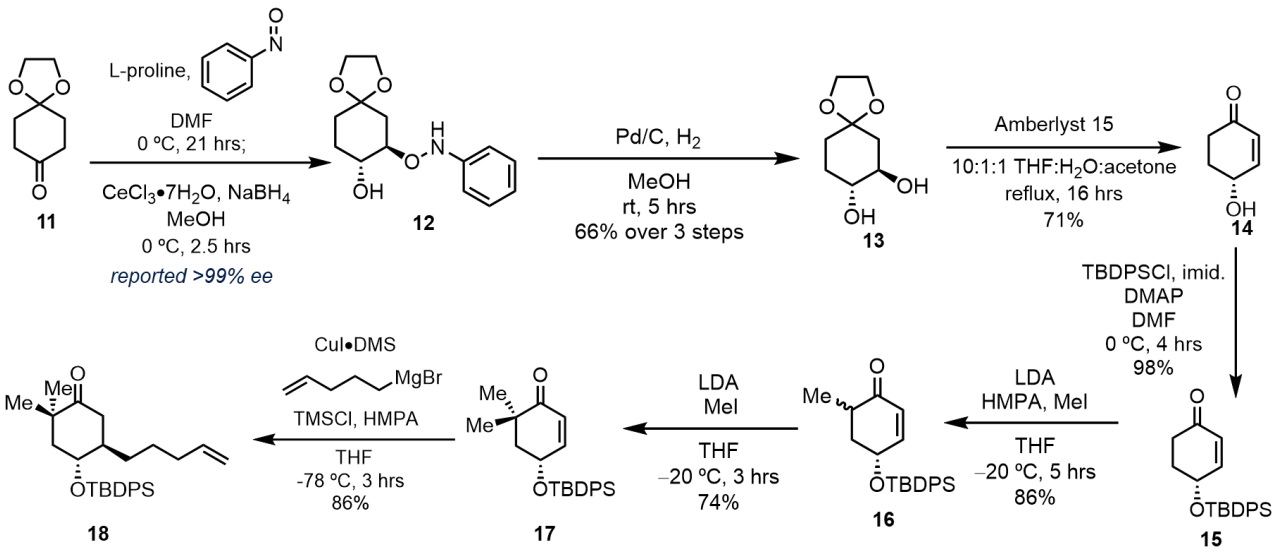

Figure 1.6: **Synthetic route to the bicyclic system, up to alkene 18**.

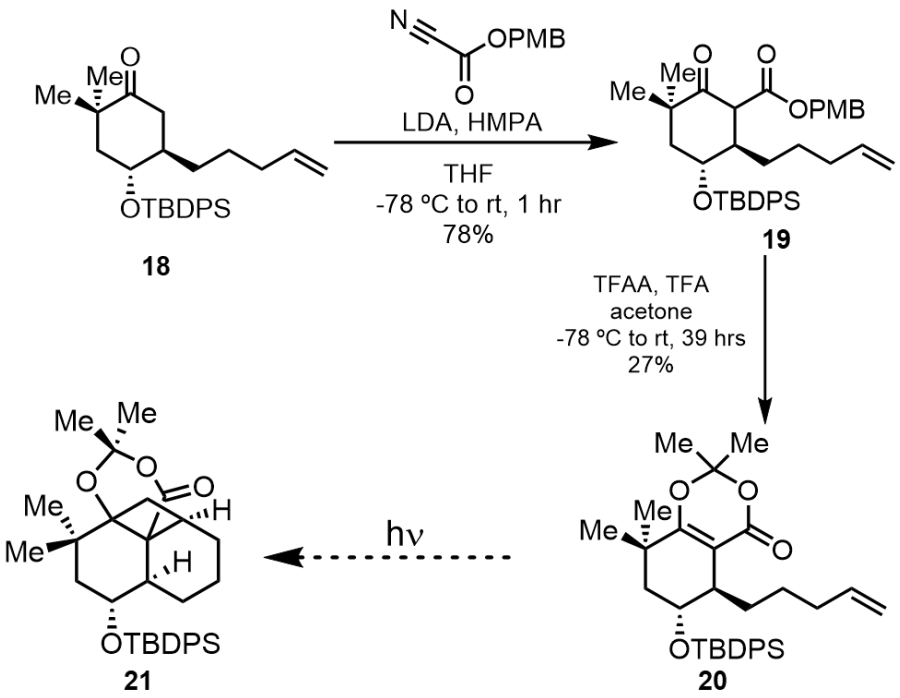

Figure 1.7: Conditions to form the prerequisite dioxenone for key photochemical reaction.

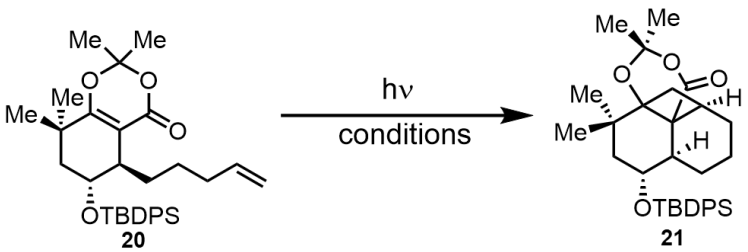

Entry	Solvent	Photosensitizer	Wavelength (nm)	Time	Yield
1	Acetonitrile	acetone	254	2 hrs	64%
2	Acetonitrile	$Ir[dF(CF_3)ppy]_2(dtbpy))PF_6$	450	>48 hrs	NR
3	DCM	$Ir[dF(CF_3)ppy]_2(dtbpy))PF_6$	450	>48 hrs	NR
4	Toluene	acetophenone	365	>48 hrs	NR
5	DCM	acetophenone	365	>48 hrs	NR
6	Toluene	fac-$[Ir(CF3\text{-}pmb)_3]$	395	>48 hrs	NR
7	Acetonitrile	benzophenone	365	>48 hrs	NR
8	DMF	$[Ru(bpy)_3]Cl_2$	365	>48 hrs	NR
9	DMF	fluoroscein	365	>48 hrs	NR

Figure 1.8: Screened photochemical conditions for [2+2] cycloaddition.

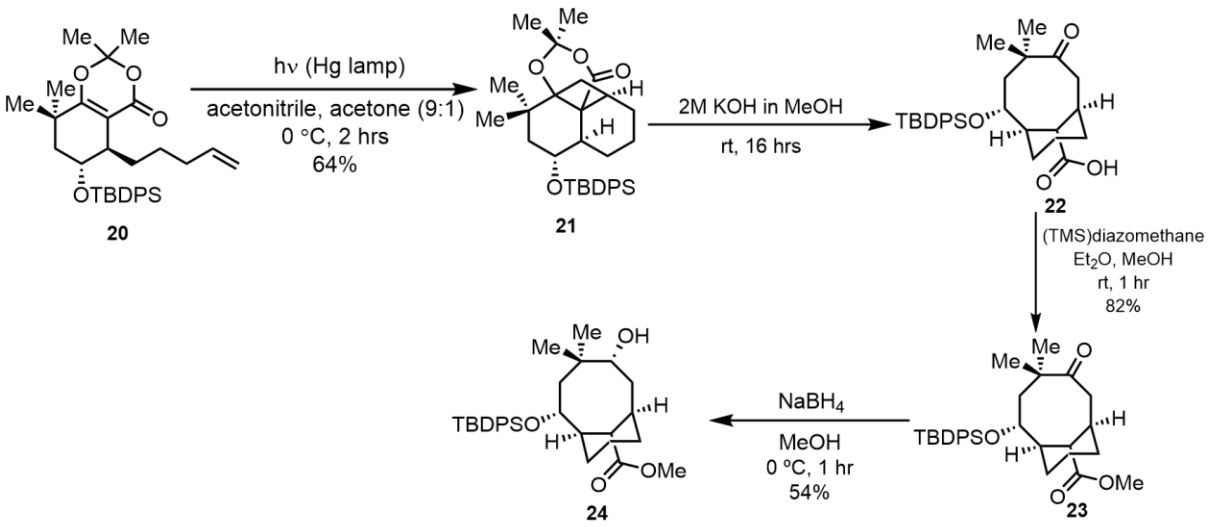

Figure 1.9: Formation of the bicyclic ring and isolation of alcohol 24.

Methods: All reactions were conducted in flame- or oven-dried glassware fitted with rubber septa under a positive pressure of nitrogen or argon, unless otherwise noted. All reaction mixtures were stirred throughout the course of each procedure using Teflon-coated magnetic stir bars. Air- and moisture-sensitive liquids were transferred via syringe or stainless-steel cannula. Solutions were concentrated by rotary evaporation below 35 °C. Analytical thin-layer chromatography (TLC) was performed using glass plates pre-coated with silica gel (0.25-mm, 60-Å pore size, 230−400 mesh, SILICYCLE INC) with a fluorescent indicator (254 nm). TLC plates were visualized by exposure to ultraviolet light (UV), and then were stained by submersion in a basic aqueous solution of with an acidic ethanolic solution of anisaldehyde, Cerium Ammonium Molybdate, followed by brief heating.

Materials: DCM, DMF, THF to be used in anhydrous reaction mixtures were dried by passage through activated alumina columns immediately prior to use. Hexanes used were ≥85% *n*-hexane. Reagents were used as received, unless otherwise noted.

Instrumentation: Unless otherwise noted, proton nuclear magnetic resonance (1H NMR) spectra and carbon nuclear magnetic resonance (13C NMR) spectra were recorded on a 400 MHz Bruker Avance III HD 2-channel instrument NMR spectrometer at 23 °C. Proton chemical shifts are expressed in parts per million (ppm, δ scale) and are referenced to residual protium in the NMR solvent (CHC13: δ 7.26, DMSO-d5: δ 2.50). Carbon chemical shifts are expressed in parts per million (ppm, δ scale) and are referenced to the carbon resonance of the NMR solvent (CDC13: δ 77.0). Data are represented as follows: chemical shift, multiplicity (s = singlet, d = doublet, t = triplet, q = quartet, dd = doublet of doublets, dt = doublet of triplets, sxt = sextet, m = multiplet, br = broad, app = apparent), integration, and coupling constant (J) in hertz (Hz).

Diol **13**

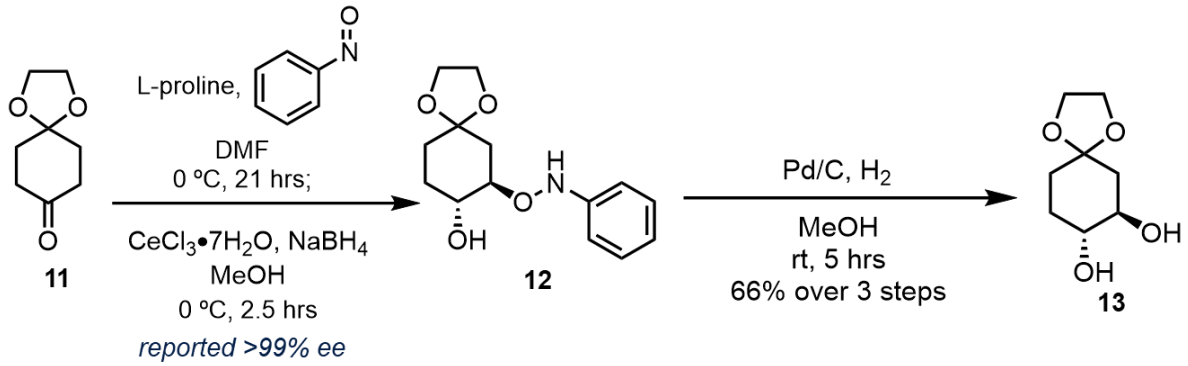

To a 500 mL RBF charged with 1,4-dioxaspiro[4.5]decan-8-one (8.75 g, 1.2 Eq, 56.0 mmol), L-proline (1.61 g, 0.3 Eq, 14.0 mmol), and a stir bar was added DMF (131 mL). The reaction vessel was cooled to 0 °C by means of an ice-water bath, and a solution of with nitrosobenzene (5.00 g, 1.0 Eq, 46.7 mmol) in DMF (58 mL) was added over 16 hours via syringe pump.

The reaction was allowed to stir for an additional 5 hours at this temperature. Methanol (116 mL) was then added, followed by cerium (III) chloride heptahydrate (24.3 g, 1.4 Eq, 65.4 mmol) in one portion. $NaBH_4$ (2.47 g, 1.4 Eq, 65.4 mmol) was then added in portions, and the reaction mixture was stirred for 2.5 hours at 0 °C (WARNING: highly exothermic! Add sodium borohydride slowly and in small portions).

The reaction mixture was then diluted with water (100 mL) and extracted with EtOAc (3 × 50 mL). The combined organic layer was washed with brine, dried over Na_2SO_4, filtered, and concentrated in vacuo to yield a red orange oil as crude. Flash chromatography of the crude material (silica gel, eluent: 30% EtOAc in hexanes) afforded the alcohol as an orange oil.

To a 250 mL RBF charged with the above alcohol and a stir bar was added 146 mL of MeOH. Pd/C (436 mg, 10% Wt, 0.00877 Eq, 410 µmol) was then added, and the reaction mixture was

stirred under a H_2 atmosphere for 5 hours. The reaction mixture was filtered through Celite and concentrated in vacuo to yield a dark brown oil as crude. Flash chromatography of the crude material (silica gel, eluent: 50% EtOAc in hexanes to 100% EtOAc) afforded diol **13** (5.38 g, 30.9 mmol, 66%) as a light brown oil.

TLC (EtOAc): Rf=0.26 (ceric ammonium molybdate)

^{1}H NMR (400 MHz, $CDCl_3$) δ 4.01 – 3.87 (m, 4H), 3.66 – 3.56 (m, 1H), 3.52 – 3.41 (m, 1H), 2.11 – 1.96 (m, 1H), 2.00 – 1.85 (m, 1H), 1.85 – 1.67 (m, 1H), 1.67 – 1.51 (m, 3H).

^{13}C NMR (100 MHz, $CDCl_3$) δ 108.84, 74.10, 72.83, 64.50, 64.39, 40.25, 32.46, 28.14.

Enone **14**

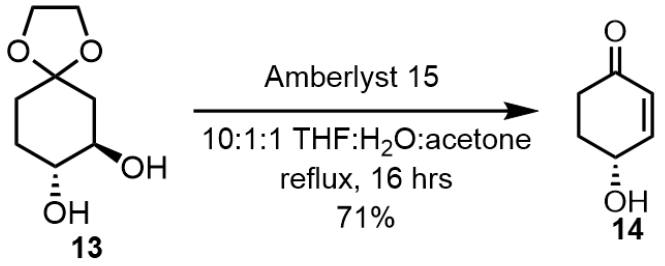

To a 250 mL RBF charged with diol **13** (1.0 g, 1 Eq, 5.7 mmol) and a stir bar was added THF (81.7 mL), water (8.17 mL), and acetone (8.17 mL). Amberlyst 15 (204 mg, 20 wt%) was added in one portion. The reaction vessel was then placed in an oil bath and allowed to heat up to 80 °C. After stirring for 16 hours at this temperature, the reaction mixture was dried over Na_2SO_4 and concentrated in vacuo to yield a brown oil as crude. Flash chromatography of the crude material (35-50% EtOAc in hexanes) afforded enone **14** (459.5 mg, 4.098 mmol, 71 %) as a light-yellow oil.

TLC (EtOAc): Rf = 0.39 (UV, anisaldehyde)

^{1}H NMR (400 MHz, $CDCl_3$) δ 6.94 (d, *J* = 2.1 Hz, 1H), 5.96 (d, *J* = 2.1 Hz, 1H), 4.57 (dd, *J* = 6.8, 2.1 Hz, 1H), 2.63 – 2.53 (m, 1H), 2.50 (br, 1H), 2.42 – 2.30 (m, 2H), 2.06 – 1.92 (m, 1H).

^{13}C NMR (100 MHz, $CDCl_3$) δ 199.11, 153.11, 129.30, 66.44, 35.48, 32.57.

TBDPS-protected enone **15**

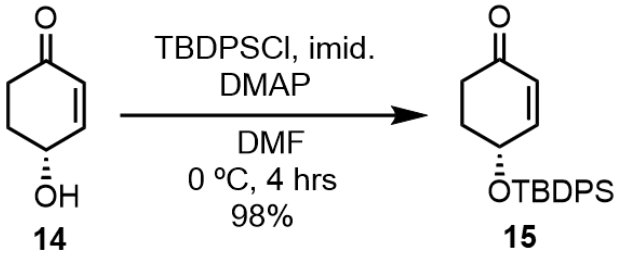

To a 500 mL RBF charged with enone **14** (1.98 g, 1 Eq, 17.7 mmol) and a stir bar was added DCM (180 mL). The reaction vessel was cooled to 0 °C by means of an ice-water bath. Imidazole (1.23 g, 1.02 Eq, 18.0 mmol) and DMAP (216 mg, 0.1 Eq, 1.77 mmol) were added each in one portion at the same temperature, followed by dropwise addition of TBDPS-Cl (4.95 g, 4.63 mL, 1.02 Eq, 18.0 mmol) via syringe. The ice-water bath was then removed, and the reaction allowed to stir at room temperature.

After stirring for 4 hours, the reaction mixture was diluted with water (200 mL) and transferred to a separatory funnel. The mixture was extracted with EtOAc (3 × 100 mL), and the combined organic layers were washed with brine, dried over sodium sulfate, and concentrated in vacuo to yield a yellow oil as crude. Flash chromatography of the crude material (silica gel, eluent: 10-20% EtOAc in hexane) afforded TBDPS-protected enone **15** (6.04 g, 17.2 mmol, 98 %) as a clear oil.

TLC (EtOAc:hexanes = 1:9): Rf = 0.26 (UV, anisaldehyde)

^{1}H NMR (400 MHz, $CDCl_3$) δ 7.76 – 7.65 (m, 5H), 7.50 – 7.35 (m, 6H), 6.79 (d, *J* = 1.2 Hz, 1H), 5.87 (d, *J* = 1.0 Hz, 1H), 4.55 – 4.46 (m, 1H), 2.58 – 2.47 (m, 1H), 2.28 – 2.13 (m, 1H), 2.13 – 2.01 (m, 2H), 1.12 – 1.02 (m, 9H).

^{13}C NMR (100 MHz, $CDCl_3$) δ 199.08, 153.39, 135.88, 135.87, 135.36, 134.93, 133.54, 133.50, 130.15, 130.13, 129.76, 128.88, 127.98, 127.94, 127.84, 77.36, 67.70, 35.46, 32.71, 26.99, 26.69, 19.28, 19.15.

Monomethylated enone **16**

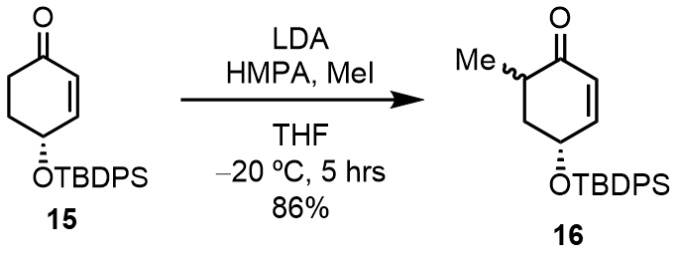

To a 100 mL RBF charged with a stir bar was added THF (34.4 mL), followed by diisopropylamine (1.18 g, 1.65 mL, 2.05 Eq, 11.7 mmol). The reaction vessel was cooled to -78 °C by means of a dry ice-acetone bath, and n-butyllithium (731 mg, 5.07 mL, 2.25 molar, 2.0 Eq, 11.4 mmol) was added dropwise. The dry ice-acetone bath was then replaced with an ice-water bath, and the reaction vessel was allowed to warm to 0 °C.

After the freshly formed LDA was allowed to stir for 30 minutes, the reaction vessel was cooled back to -78°C by means of a dry ice-acetone bath. A solution of TBDPS-protected enone **15** (2.00 g, 1 Eq, 5.71 mmol) in THF (6.8 mL) was then added dropwise. After allowing the solution to stir for 30 minutes, HMPA (10.2 g, 9.93 mL, 10.0 Eq, 57.1 mmol) and methyl iodide (4.05 g, 1.78 mL, 5.0 Eq, 28.5 mmol) were added in succession.

After stirring at -78°C for 5 minutes, the dry ice-acetone bath was replaced with an ice-salt bath (-20 °C). After stirring for 5 hours at this temperature, the reaction was quenched by the addition of aqueous saturated NH_4Cl (50 mL). The organic layer was collected, and the aqueous layer was extracted with EtOAc (3 × 50 mL). The combined organic layers were washed with brine (50 mL), dried over sodium sulfate, and concentrated in vacuo. Flash chromatography of the crude material (silica gel, eluent: 0-5% EtOAc in hexanes) afforded monomethylated enone **16** (1.794 g, 4.921 mmol, 86 %) as a colorless oil and an inseparable 1.5:1 mixture of diastereomers.

TLC (EtOAc:hexanes = 1:9): Rf = 0.35 (UV, anisaldehyde)

^{1}H NMR (400 MHz, $CDCl_3$, integration of 1 per H for minor diastereomer, 1.5 per H for major diastereomer) δ 7.81 – 7.58 (m, 10H), 7.54 – 7.33 (m, 15H), 6.77 (dt, *J* = 10.2, 2.0 Hz, 1H), 6.62 (dd, *J* = 10.1, 4.1 Hz, 1.5H), 5.96 – 5.79 (m, 2.5H), 4.64 – 4.50 (m, 1H), 4.44 (app q, *J* = 4.5 Hz, 1.5H), 2.91 – 2.75 (m, 1.5H), 2.26 – 2.02 (m, 3.5H), 1.92 – 1.74 (m, 2.5H), 1.16 – 0.96 (m, 30H).

^{13}C NMR (100 MHz, $CDCl_3$) δ 202.41, 201.22, 153.69, 148.84, 135.89, 135.88, 135.86, 133.73, 133.61, 133.58, 133.52, 130.13, 130.10, 128.75, 128.41, 127.98, 127.94, 127.92, 68.97, 64.80, 41.71, 40.21, 39.25, 37.75, 27.03, 27.00, 19.34, 19.25, 15.19, 15.12.

Dimethylated enone **17**

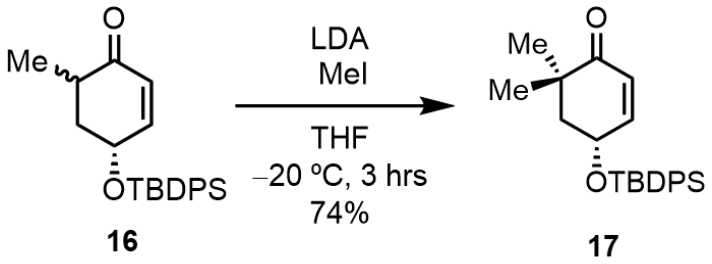

To a 50 mL RBF charged with a stir bar was added THF (15 mL), followed by diisopropylamine (361 mg, 503 µL, 1.3 Eq, 3.57 mmol). The reaction vessel was cooled to -78 °C by means of a dry ice-acetone bath, and n-butyllithium (1.62 mL, 2.03 molar, 1.2 Eq, 3.29 mmol) was added dropwise. The dry ice-acetone bath was then replaced with an ice-water bath, and the reaction vessel was allowed to warm to 0 °C.

After the freshly formed LDA was allowed to stir for 30 minutes, the reaction vessel was cooled back to -78 °C by means of a dry ice-acetone bath. A solution of monomethylated enone **16** (1.00 g, 1 Eq, 2.74 mmol) in THF (5.6 mL) was then added dropwise. After allowing the solution to stir for 30 minutes, methyl iodide (4.05 g, 1.78 mL, 5.0 Eq, 28.5 mmol) was added.

After stirring at -78 °C for 5 minutes, the dry ice-acetone bath was replaced with an ice-salt bath (-20°C). After stirring for 2 hours at this temperature, the reaction was quenched by the addition of saturated aqueous NH_4Cl (30 mL). The organic layer was collected, and the aqueous layer was extracted with EtOAc (3 × 30 mL). The combined organic layers were washed with brine, dried over sodium sulfate, and concentrated in vacuo. Flash chromatography of the crude material (silica gel, eluent: 0-5% EtOAc in hexanes) afforded dimethylated enone **17** (763.1 mg, 2.016 mmol, 74%) as a colorless oil.

TLC (EtOAc:hexanes = 1:9): Rf = 0.46 (UV, anisaldehyde)

^{1}H NMR (400 MHz, $CDCl_3$) δ 7.75 – 7.68 (m, 4H), 7.54 – 7.39 (m, 6H), 6.75 (dt, *J* = 10.2, 2.0 Hz, 1H), 5.80 (dd, *J* = 10.3, 2.1 Hz, 1H), 4.59 (ddt, *J* = 9.6, 5.0, 2.1 Hz, 1H), 1.99 (dd, *J* = 13.0, 9.5 Hz, 1H), 1.90 – 1.81 (m, 1H), 1.14 – 1.08 (m, 12H), 0.89 (s, 3H).

^{13}C NMR (100 MHz, $CDCl_3$) δ 203.88, 151.83, 135.92, 135.90, 133.61, 130.13, 127.96, 127.91, 127.27, 66.77, 46.45, 42.02, 27.03, 25.79, 24.28, 19.25.

Alkene **18**

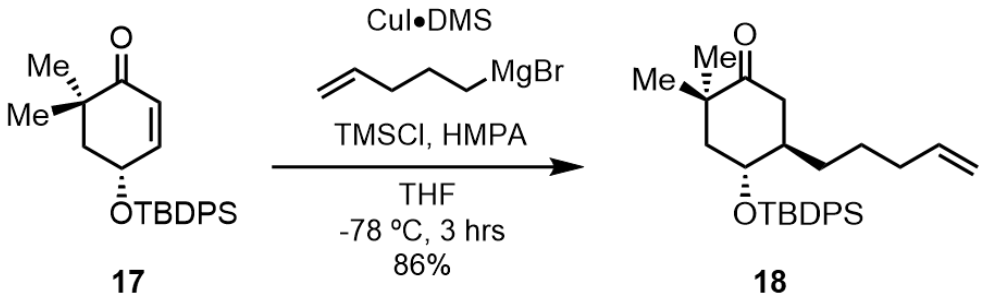

To a 100 mL three-neck RBF charged with a stir bar was added magnesium (423 mg, 17.46 mmol), followed by THF (2.1 mL). To the rapidly stirring suspension was added 1,2-dibromoethane (75.3 µL, 873 µmol) dropwise. A solution of 5-bromopent-1-ene (1.38 mL, 11.64 mmol) in THF (9 mL) was then added dropwise, and the suspension was allowed to stir for an additional 1 hour. The suspension was allowed to settle, and the resulting Grignard solution was titrated against a solution of I_2 in 0.5 molar LiCl in THF to yield the concentration as 0.8 molar.

To a 25 mL RBF charged with copper(I) iodide (369 mg, 1.0 Eq, 1.94 mmol) and a stir bar was added THF (6.6 mL), methyl sulfide (0.66 mL), and HMPA (810 µL, 2.4 Eq, 4.65 mmol). The reaction vessel was cooled to -78 °C by means of a dry ice-acetone bath, and the Grignard solution (4.85 mL, 0.80 molar, 2.0 Eq, 3.88 mmol) was added dropwise. After stirring for 1 hour at this temperature, a solution of dimethylated enone **17** (734 mg, 1.0 Eq, 1.94 mmol) and TMS-Cl (492 µL, 2.0 Eq, 3.88 mmol) in THF (4.4 mL) was added dropwise over 1 hour via syringe pump. The reaction mixture was allowed to stir at this temperature for an additional 3 hours, at room temperature for 15 minutes, and then quenched with acetic acid (0.44 mL). After stirring for an additional 12 hrs, saturated aqueous NH_4Cl (30 mL) was added. The organic layer was collected, and the aqueous layer was extracted with EtOAc (3 × 30 mL). The combined organic layers were washed with brine (30 mL), dried over sodium sulfate, and concentrated in vacuo. Flash

chromatography of the crude material (silica gel, eluent: 0-5% EtOAc in hexanes) afforded alkene **18** (747.1 mg, 1.665 mmol, 86%) as a colorless oil and a 5:1 mixture of diastereomers. A small portion of this material was carefully purified by column chromatography for characterization purposes.

TLC (EtOAc:hexanes = 1:9): Rf = 0.53 (UV, anisaldehyde)

^{1}H NMR (400 MHz, $CDCl_3$) δ 7.74 – 7.65 (m, 4H), 7.49 – 7.34 (m, 6H), 5.78 – 5.63 (m, 1H), 5.00 – 4.87 (m, 2H), 3.84 (td, *J* = 7.3, 4.5 Hz, 1H), 2.66 (dd, *J* = 14.4, 4.8 Hz, 1H), 2.13 – 2.02 (m, 1H), 2.01 – 1.78 (m, 3H), 1.73 – 1.48 (m, 4H), 1.33 – 1.19 (m, 2H), 1.19 – 0.94 (m, 12H), 0.92 – 0.82 (m, 3H).

^{13}C NMR (100 MHz, $CDCl_3$) δ 215.52, 138.66, 136.13, 136.08, 134.34, 133.83, 129.98, 129.84, 127.80, 127.70, 114.73, 71.67, 46.34, 45.53, 44.75, 40.16, 33.82, 31.93, 27.21, 26.57, 25.81, 25.58, 19.50.

Beta keto ester **19**

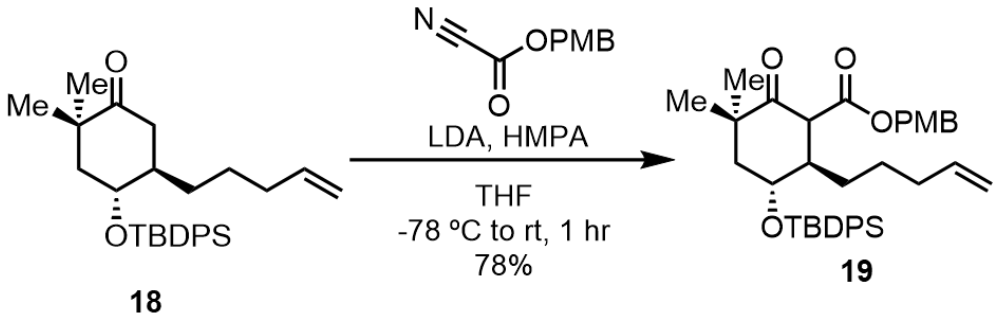

To a 25 mL RBF charged with a stir bar was added THF (5.33 mL), followed by diisopropylamine (169 µL, 1.50 Eq, 1.200 mmol). The reaction vessel was cooled to -78 °C by means of a dry ice-acetone bath, and n-butyllithium (526.6 µL, 2.02 molar, 1.33 Eq, 1.064 mmol) was added dropwise. The dry ice-acetone bath was then replaced with an ice-water bath, and the reaction vessel was allowed to warm to 0 °C.

After the freshly formed LDA was allowed to stir for 30 minutes, the reaction vessel was cooled back to -78 °C by means of a dry ice-acetone bath. A solution of alkene **18** (358.9 mg, 1.0 Eq, 799.8 µmol) in THF (1.5 mL) was added dropwise. The reaction mixture was allowed to stir at this temperature for 30 minutes. A solution of HMPA (139 µL, 1.00 Eq, 799.8 µmol) and anisyl cyanoformate (203.4 mg, 1.33 Eq, 1.064 mmol) in THF (1.5 mL) was added in one portion. After stirring at this temperature for 1 hour, the reaction mixture was partitioned between water (5 mL) and ethyl acetate (5 mL). The organic layer was collected and washed with water (10 mL). The organic layer was then dried over sodium sulfate and concentrated in vacuo. Flash chromatography of the crude material (silica gel, eluent: 0-5% EtOAc in hexanes) afforded beta keto ester **19** (382.4 mg, 623.9 µmol, 78 %) as a colorless oil.

TLC (EtOAc:hexanes = 1:9): Rf = 0.56 (UV, anisaldehyde)

Dioxenone **20**

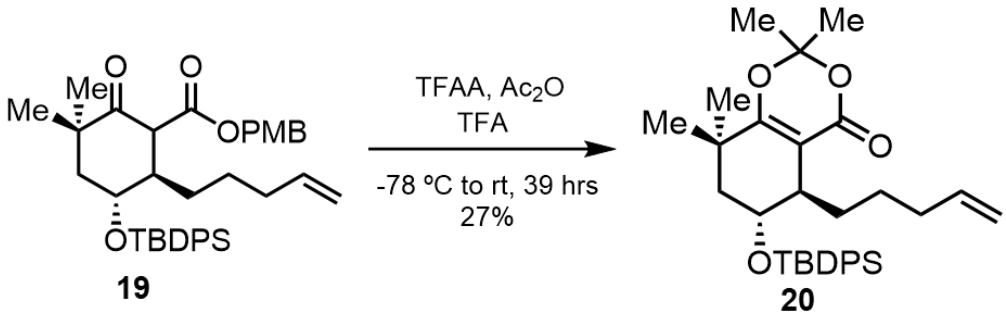

To a 25 mL RBF charged with beta keto ester **19** (563.1 mg, 1 Eq, 918.8 μmol) and a stir bar was added acetone (6.07 mL). The reaction vessel was cooled to -78°C by means of a dry ice-acetone bath, and trifluoroacetic anhydride (1.3 mL) was added dropwise. After stirring at this temperature for 30 minutes, trifluoroacetic acid (4.6 mL) was added dropwise. The dry ice-acetone bath was then removed, and the reaction mixture was allowed to warm to room temperature. After stirring for 39 hours, the resulting reaction mixture was concentrated in vacuo and azeotroped with toluene (3 × 10 mL). Flash chromatography of the crude material (silica gel, eluent: 0-5% EtOAc in hexanes) afforded dioxenone **20** (131.6 mg, 247.0 μmol, 27%) as a yellow oil.

^{1}H NMR (300 MHz, $CDCl_3$) δ 7.76 – 7.52 (m, 4H), 7.50 – 7.32 (m, 6H), 5.67 – 4.49 (m, 1H), 4.96 – 4.73 (m, 2H), 3.96 – 3.84 (m, 1H), 2.67 – 2.46 (m, 1H), 1.89 – 1.67 (m, 3H), 1.72 (s, 3H), 1.71 – 1.67 (m, 1H), 1.64 (s, 3H), 1.62 – 1.55 (m, 1H), 1.52 – 1.36 (m, 1H), 1.33 (s, 3H), 1.15 – 0.93 (m, 9H), 1.01 (s, 3H), 0.85 – 0.70 (m, 2H).

Photoadduct **21**

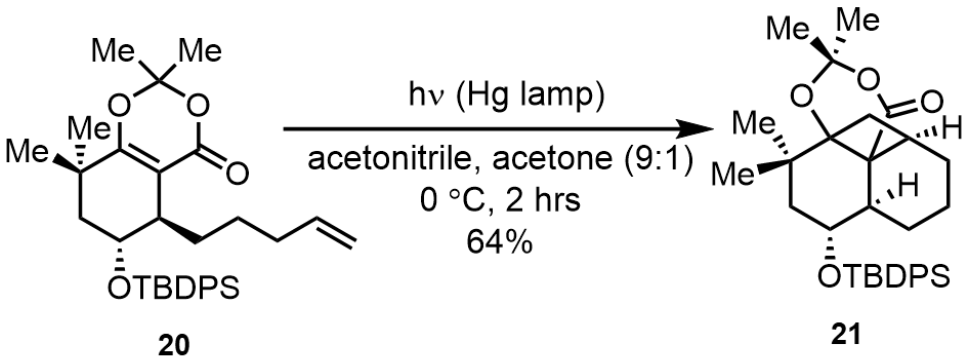

20 **21**

To a 20 mL microwave vial charged with dioxenone **20** (75.0 mg, 1 Eq, 141 μmol) and a stir bar was added acetonitrile (16.74 mL) and acetone (1.86 mL). The resulting solution was sparged with argon for 30 minutes, and then irradiated using a 450W Hanovia medium pressure lamp for 2 hours. The reaction solution was then concentrated in vacuo. Flash chromatography of the crude material (silica gel, eluent: 0-5% EtOAc in hexanes) afforded photoadduct **21** (48.0 mg, 90.1 μmol, 64%) as a colorless oil and as a 2:1 mixture of isomers.

Methyl ester **23**

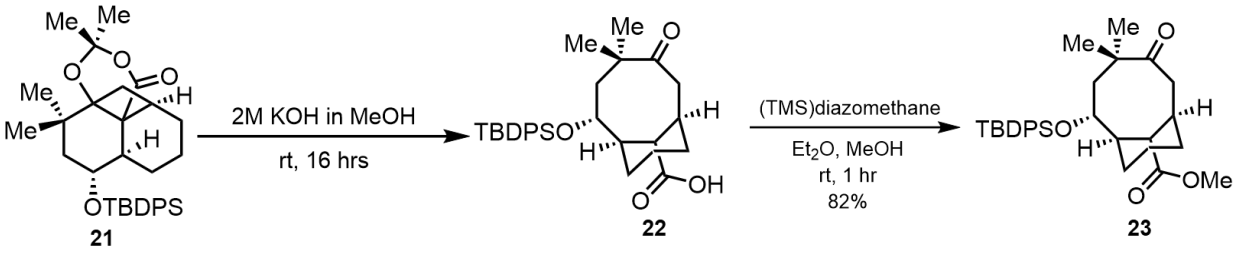

To a 10 mL RBF charged with photoadduct **21** (35.6 mg, 1 Eq, 66.8 μmol) and a stir bar was added 2N KOH/MeOH (1.48 mL). After stirring for 55 hours at 25 °C, the reaction solution was diluted with water and extracted with EtOAc. The organic layer was then washed with 2 N aqueous HCl, and the acidic aqueous layer was washed again with EtOAc (3 × 10 mL). The combined organic layers were then dried over sodium sulfate and concentrated in vacuo. The resulting crude carboxylic acid was carried forward to the next reaction without further purification.

To a 10 mL RBF charged with crude carboxylic acid and a stir bar was added 0.32 mL of ethyl ether and 0.19 mL of methanol. TMS-diazomethane (102 μL, 1.8 molar in hexanes, 3.0 Eq, 183 μmol) was added dropwise, and the reaction was allowed to stir for 1 hour at 25 °C. The reaction mixture was then concentrated in vacuo. Flash chromatography of the crude material (silica gel, eluent: 0-5% EtOAc in hexanes) afforded methyl ester **23** (25.3 mg, 49.9 μmol, 82%) as a colorless oil and an inseparable mixture of diastereomers.

Alcohol **24**

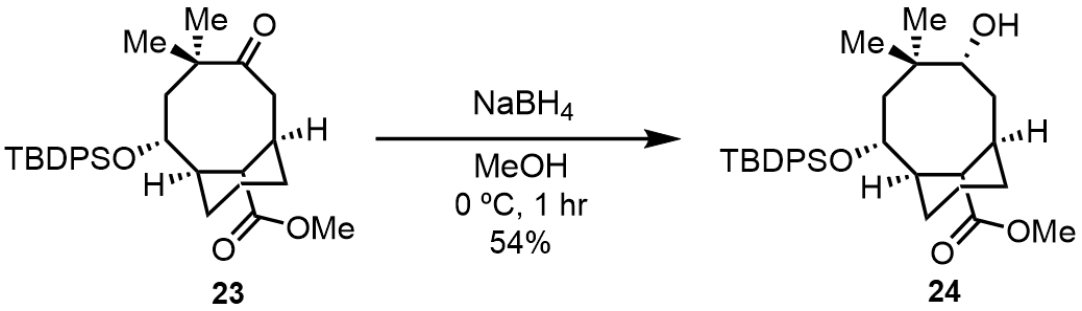

23 **24**

To a 10 mL RBF charged with methyl ester **23** (25.3 mg, 1 Eq, 49.9 μmol) and a stir bar was added methanol (1 mL). The reaction vessel was cooled to 0 °C by means of an ice-water bath, and NaBH4 (1 mg, 0.5 Eq, 25 μmol) was added. The reaction mixture was allowed to stir at this temperature for 1 hour, and then water was added to quench the reaction. The reaction mixture was washed with EtOAc (3 × 10 mL), and the combined organic layers were dried over sodium sulfate and concentrated in vacuo. Flash chromatography of the crude material (silica gel, eluent: 20% EtOAc in hexanes) afforded alcohol **24** (13.8 mg, 27.1 μmol, 54%) as a colorless oil.

^{1}H NMR (400 MHz, C_6D_6) δ 7.89 – 7.77 (m, 4H), 7.24 – 7.16 (m, 6H), 4.29 – 4.18 (m, 1H), 3.69 (s, 1H), 3.36 (s, 3H), 2.98 (t, *J* = 5.1 Hz, 1H), 2.81 (s, 1H), 2.62 (s, 1H), 2.27 (dd, *J* = 15.2, 9.1 Hz, 1H), 1.98 – 1.85 (m, 2H), 1.80 – 1.61 (m, 3H), 1.17 (s, 9H), 1.10 – 1.01 (m, 3H), 1.00 – 0.89 (m, 4H), 0.72 (s, 3H), 0.56 (s, 3H).

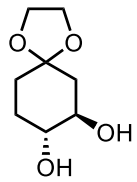

13

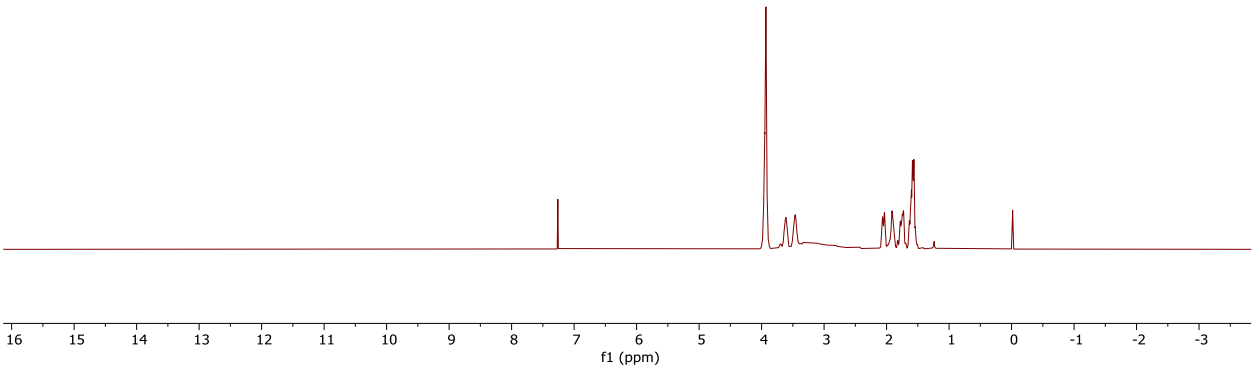

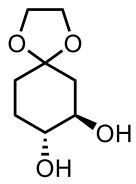
O
O
OH
OH

13

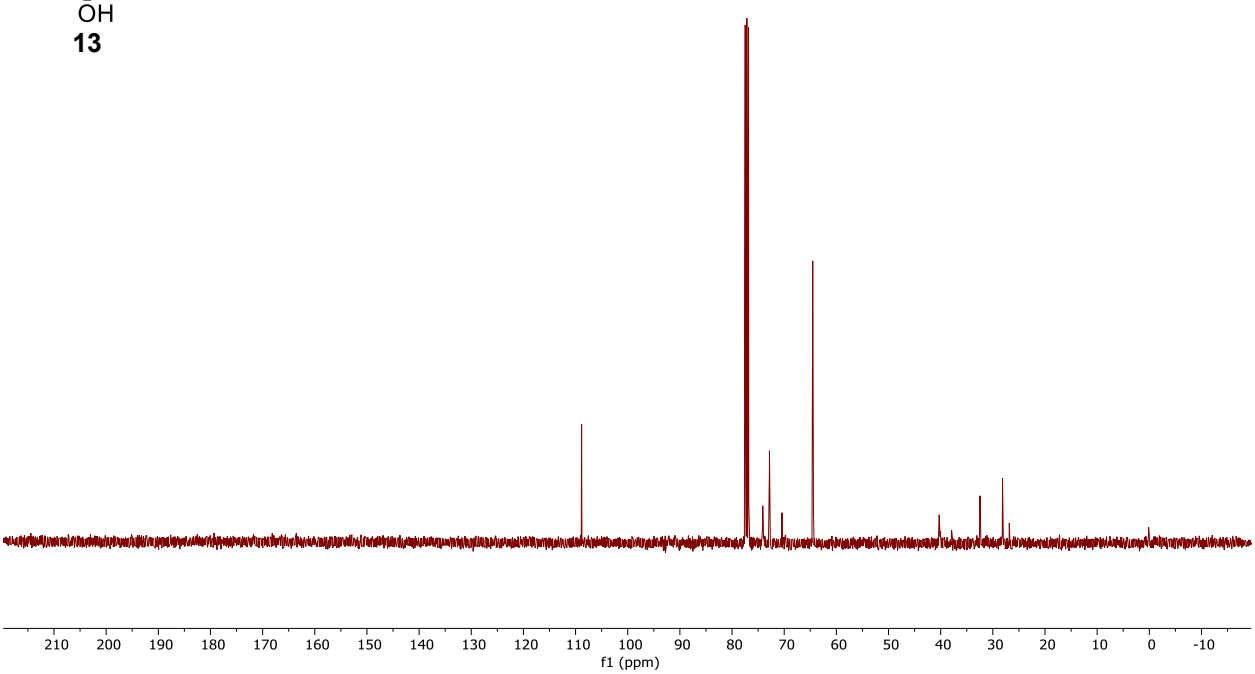
210
200
190
180
170
160
150
140
130
120
110
100
90
80
70
60
50
40
30
20
10
0
-10
f1 (ppm)

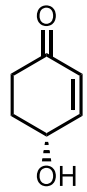
O
OH

14

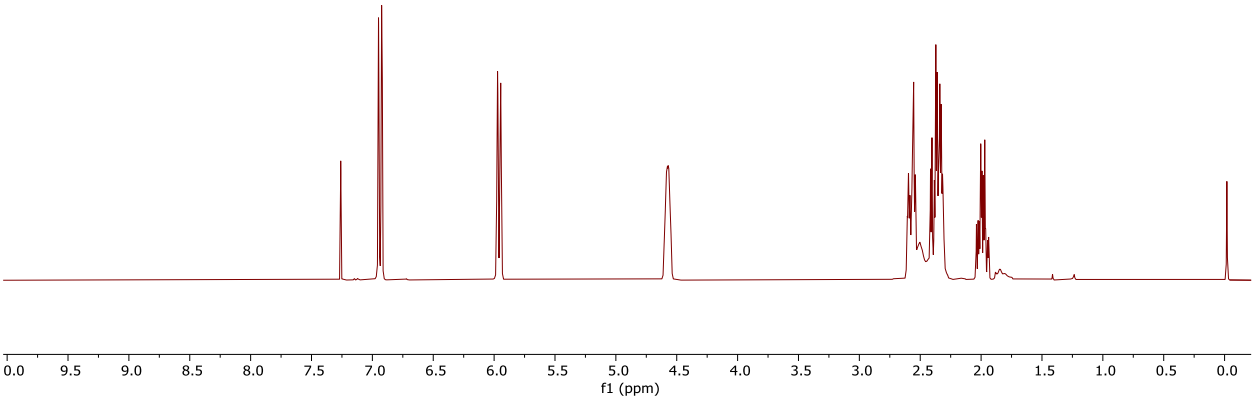
0.0
9.5
9.0
8.5
8.0
7.5
7.0
6.5
6.0
5.5
5.0
4.5
4.0
3.5
3.0
2.5
2.0
1.5
1.0
0.5
0.0
f1 (ppm)


O
OH

14

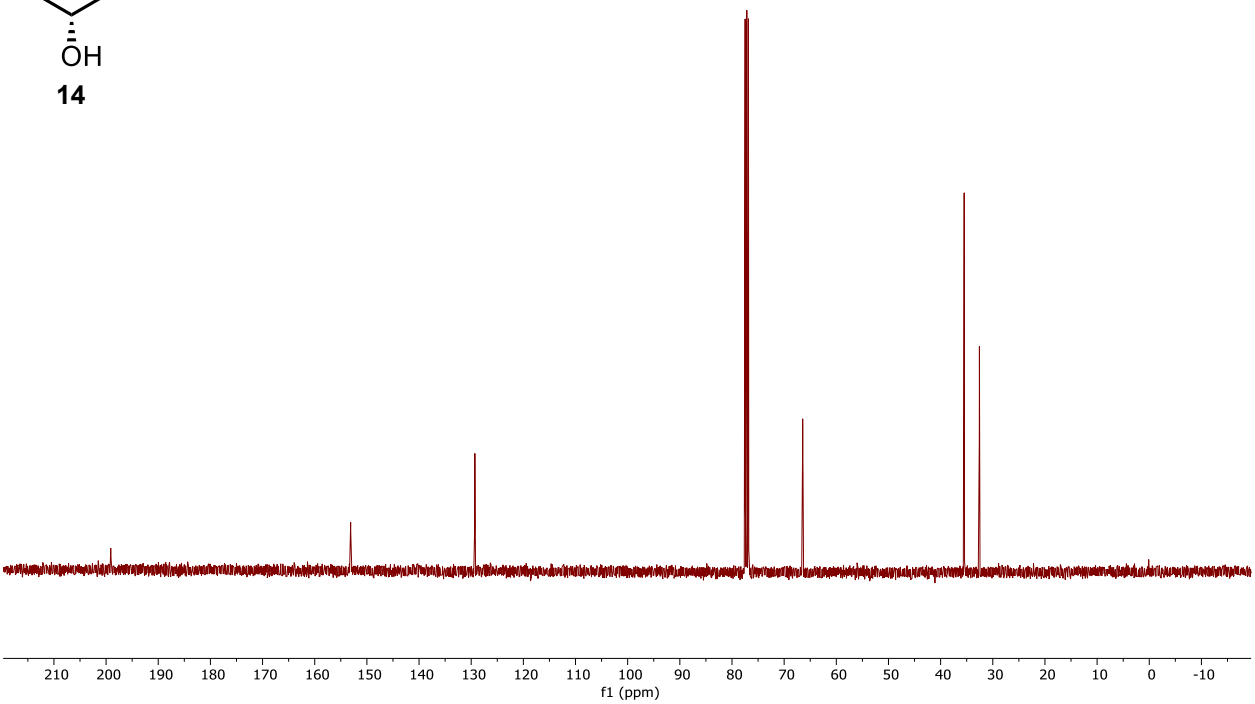
210
200
190
180
170
160
150
140
130
120
110
100
90
80
70
60
50
40
30
20
10
0
-10
f1 (ppm)

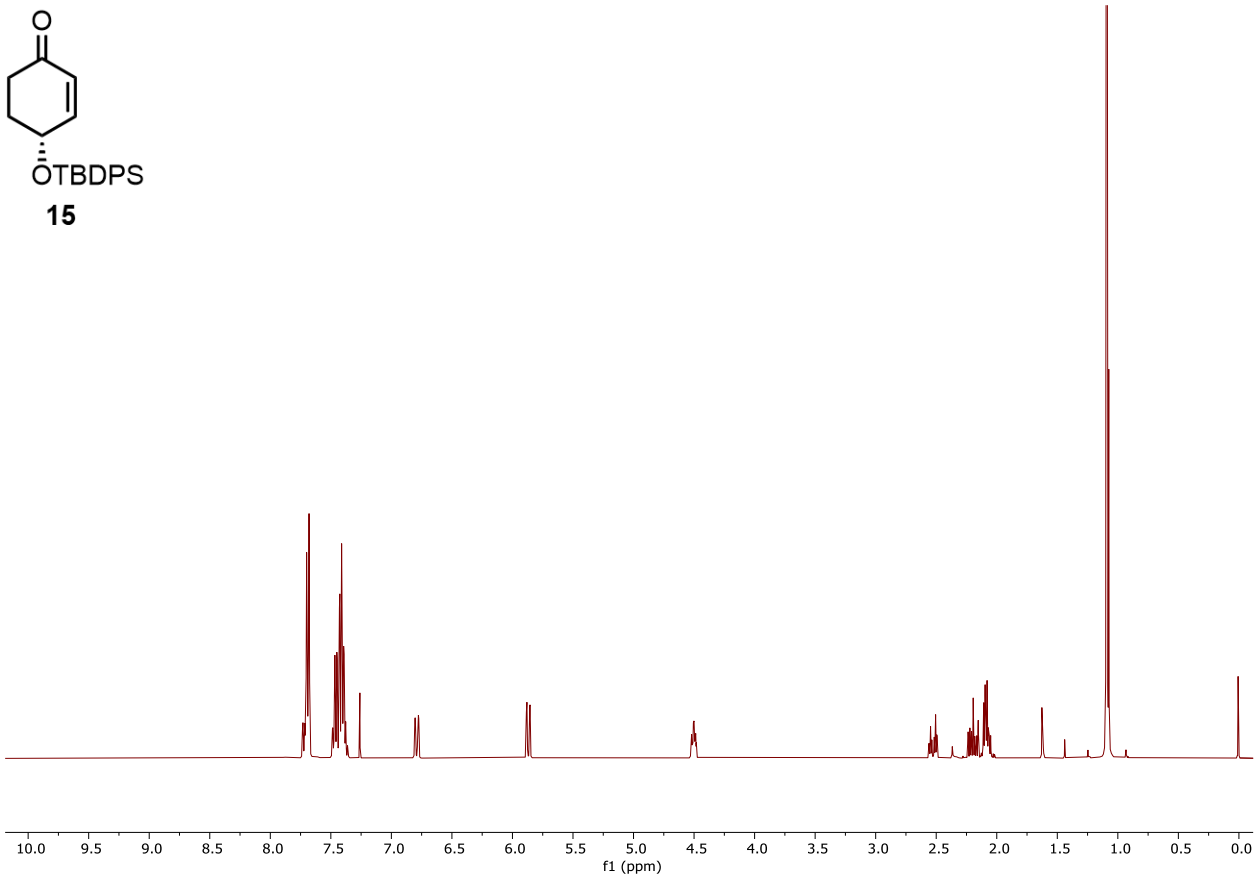
O
OTBDPS
15
10.0
9.5
9.0
8.5
8.0
7.5
7.0
6.5
6.0
5.5
5.0
4.5
4.0
3.5
3.0
2.5
2.0
1.5
1.0
0.5
0.0
f1 (ppm)

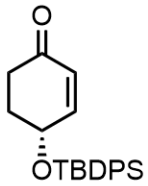
O
OTBDPS

15

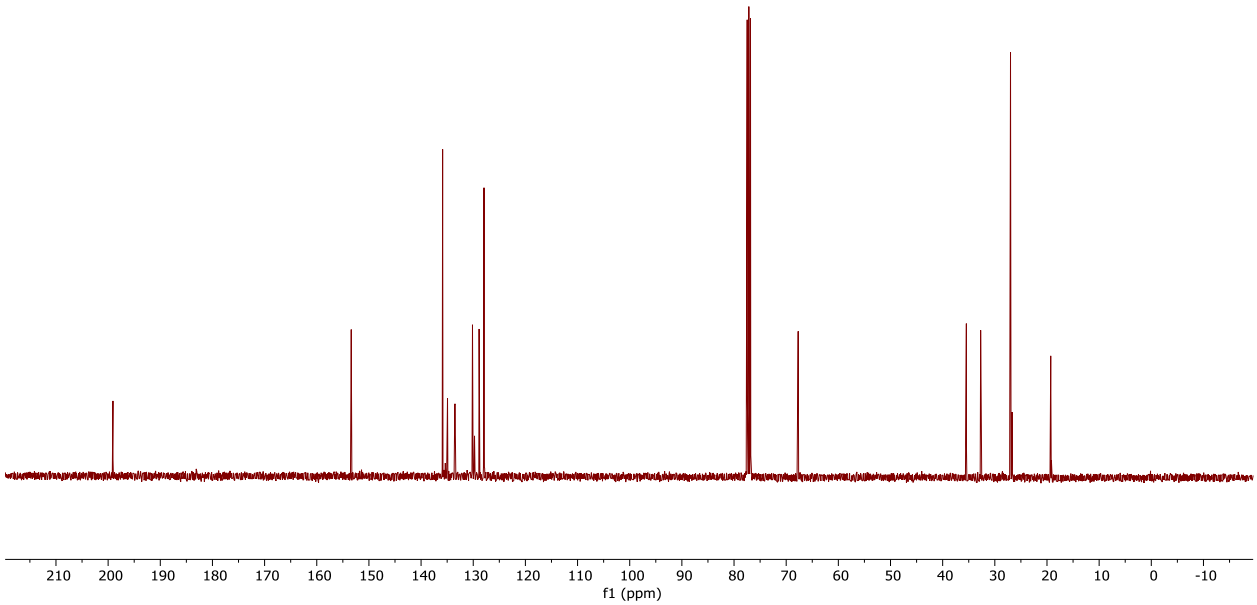
210
200
190
180
170
160
150
140
130
120
110
100
90
80
70
60
50
40
30
20
10
0
-10
f1 (ppm)

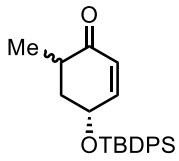
O
Me
OTBDPS

16

10.0
9.5
9.0
8.5
8.0
7.5
7.0
6.5
6.0
5.5
5.0
4.5
4.0
3.5
3.0
2.5
2.0
1.5
1.0
0.5
0.0
f1 (ppm)

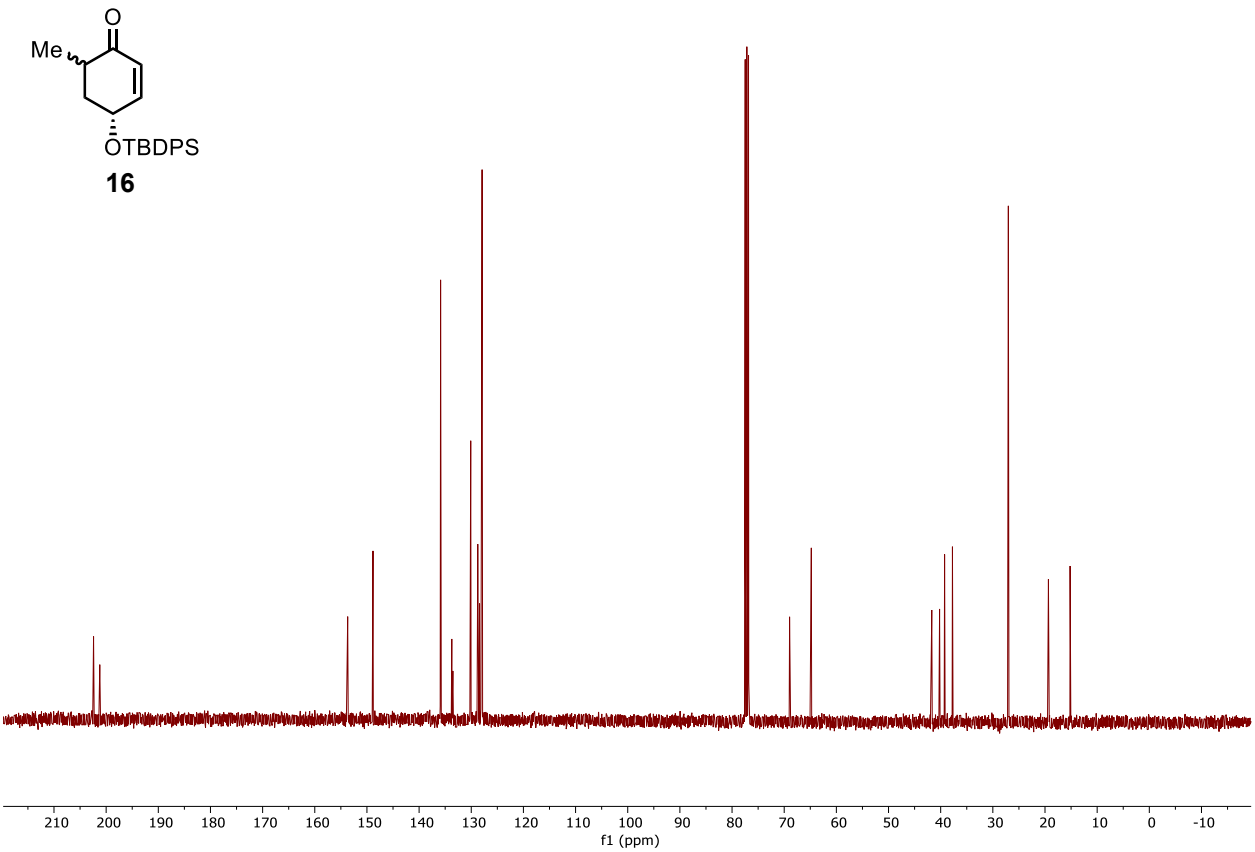
O
Me
OTBDPS
16
210 200 190 180 170 160 150 140 130 120 110 100 90 80 70 60 50 40 30 20 10 0 -10
f1 (ppm)

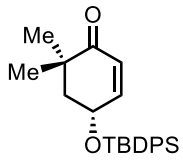
O
Me
Me
OTBDPS

17

9.5
9.0
8.5
8.0
7.5
7.0
6.5
6.0
5.5
5.0
4.5
4.0
3.5
3.0
2.5
2.0
1.5
1.0
0.5
0.0
f1 (ppm)

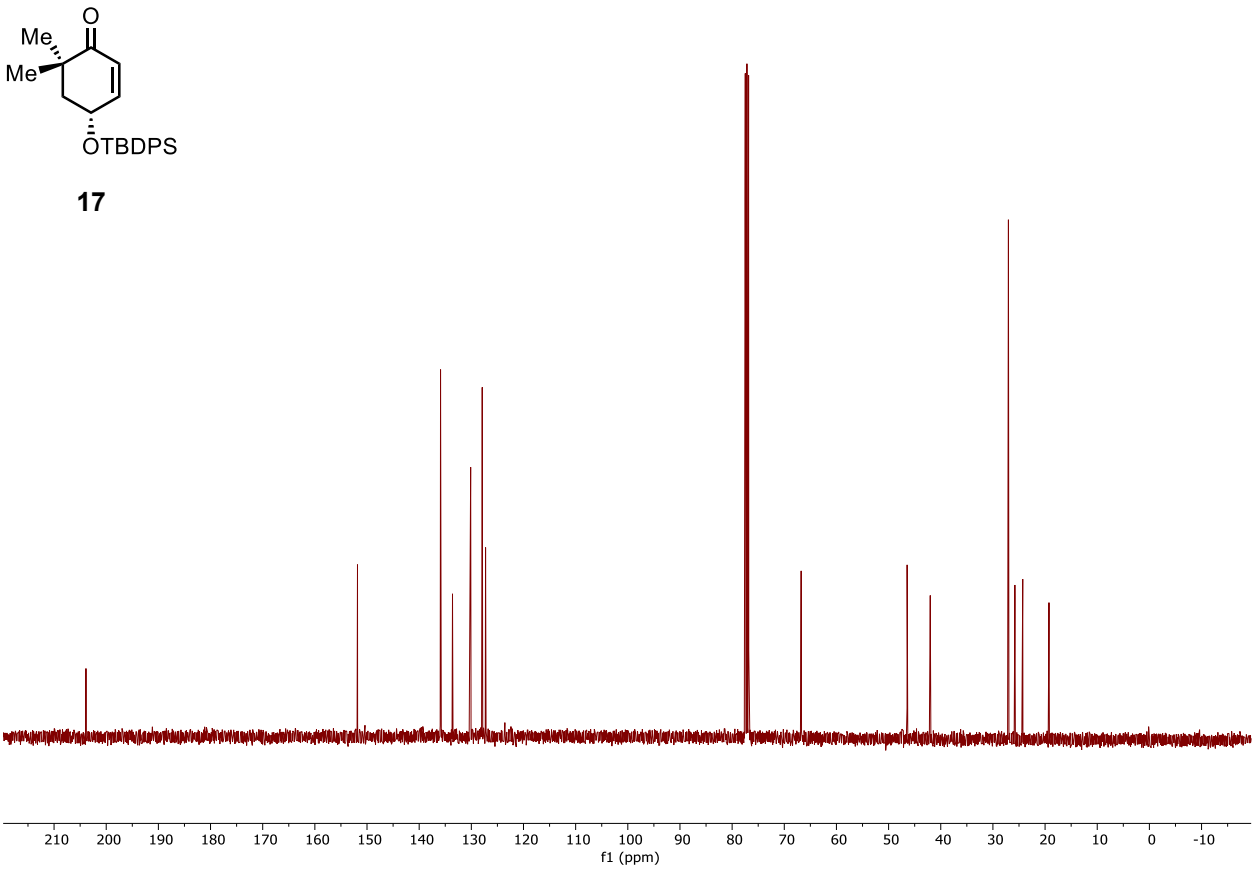
O
Me
Me
OTBDPS
210 200 190 180 170 160 150 140 130 120 110 100 90 80 70 60 50 40 30 20 10 0 -10
f1 (ppm)

17

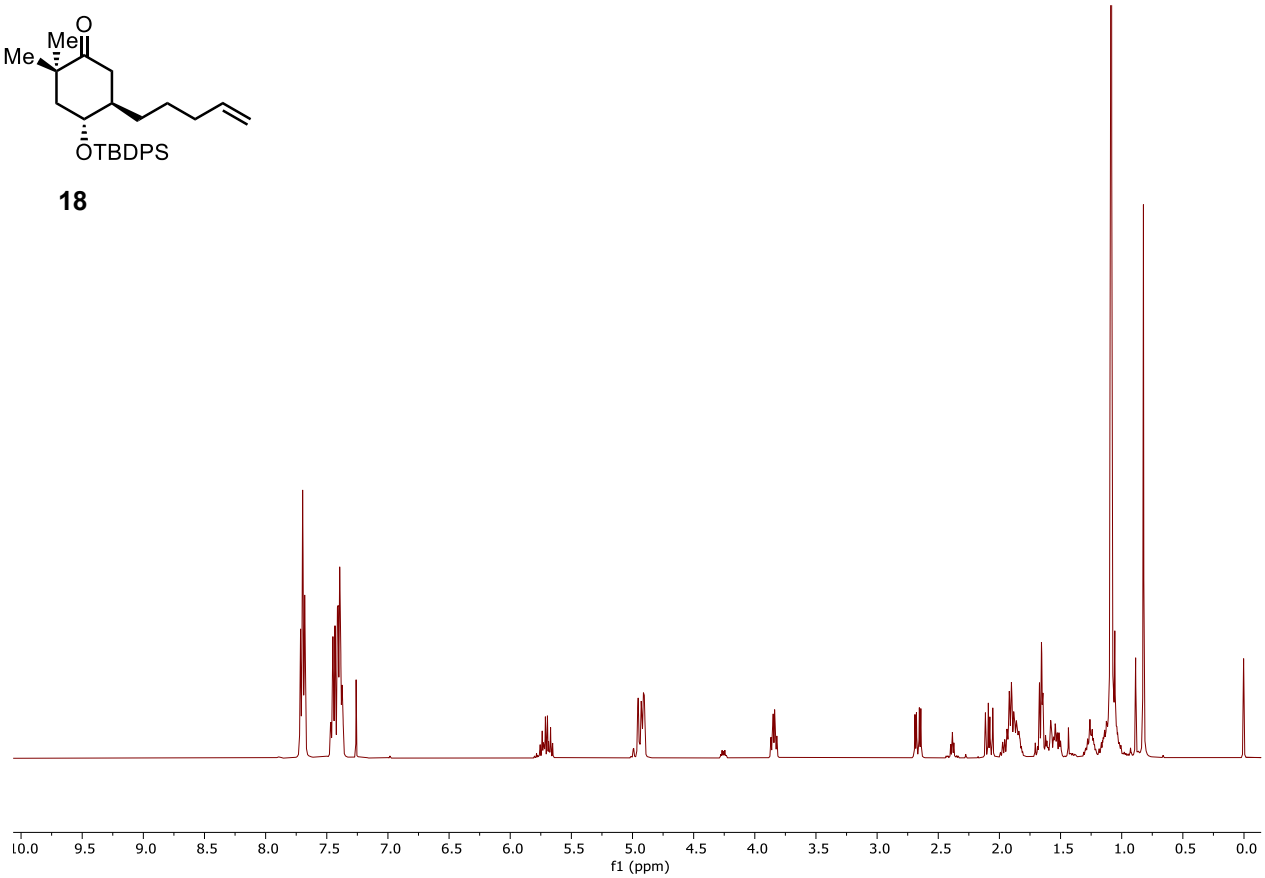
O
Me
Me
OTBDPS
10.0
9.5
9.0
8.5
8.0
7.5
7.0
6.5
6.0
5.5
5.0
4.5
4.0
3.5
3.0
2.5
2.0
1.5
1.0
0.5
0.0
f1 (ppm)

18

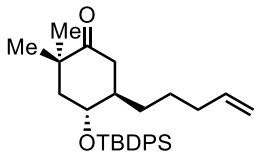
O
Me
Me
OTBDPS

18

210
200
190
180
170
160
150
140
130
120
110
100
90
80
70
60
50
40
30
20
10
0
-10
f1 (ppm)

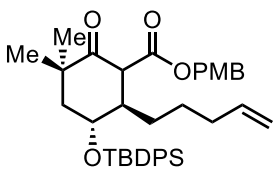
O
O
Me
Me
OPMB
OTBDPS

19

5.0 14.5 14.0 13.5 13.0 12.5 12.0 11.5 11.0 10.5 10.0 9.5 9.0 8.5 8.0 7.5 7.0 6.5 6.0 5.5 5.0 4.5 4.0 3.5 3.0 2.5 2.0 1.5 1.0 0.5 0.0
f1 (ppm)

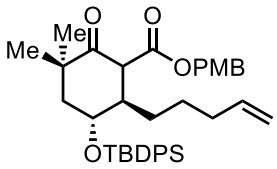
Me
O
Me
O
OPMB
OTBDPS

19

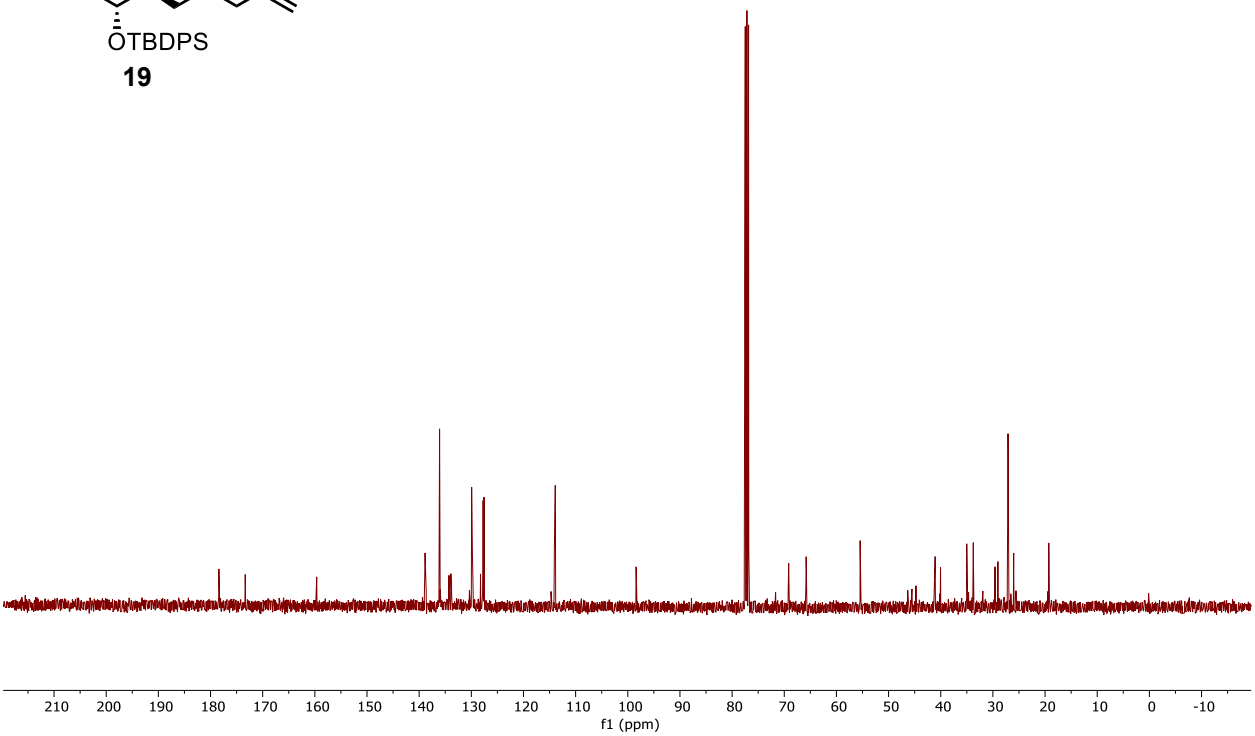
210
200
190
180
170
160
150
140
130
120
110
100
90
80
70
60
50
40
30
20
10
0
-10
f1 (ppm)

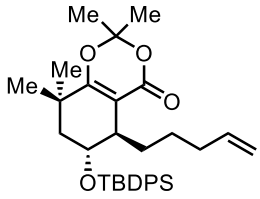
Me
Me
O
O
Me
Me
O
OTBDPS

20

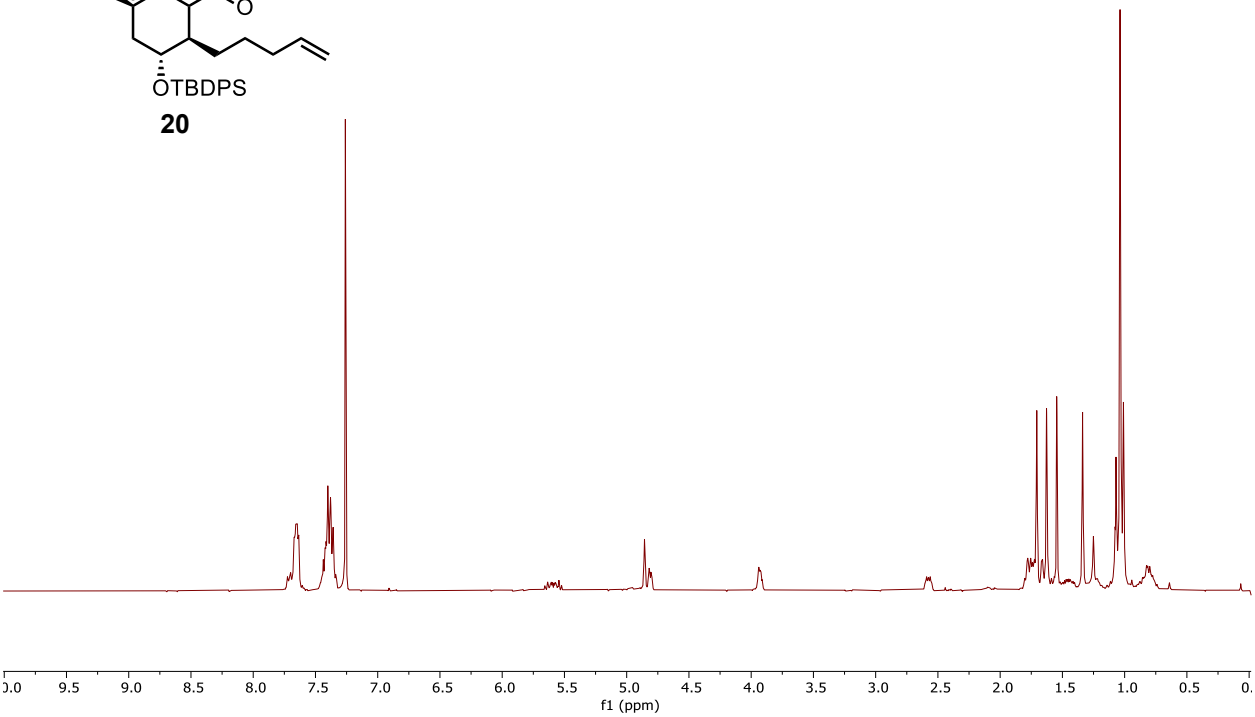
9.5
9.0
8.5
8.0
7.5
7.0
6.5
6.0
5.5
5.0
4.5
4.0
3.5
3.0
2.5
2.0
1.5
1.0
0.5
f1 (ppm)

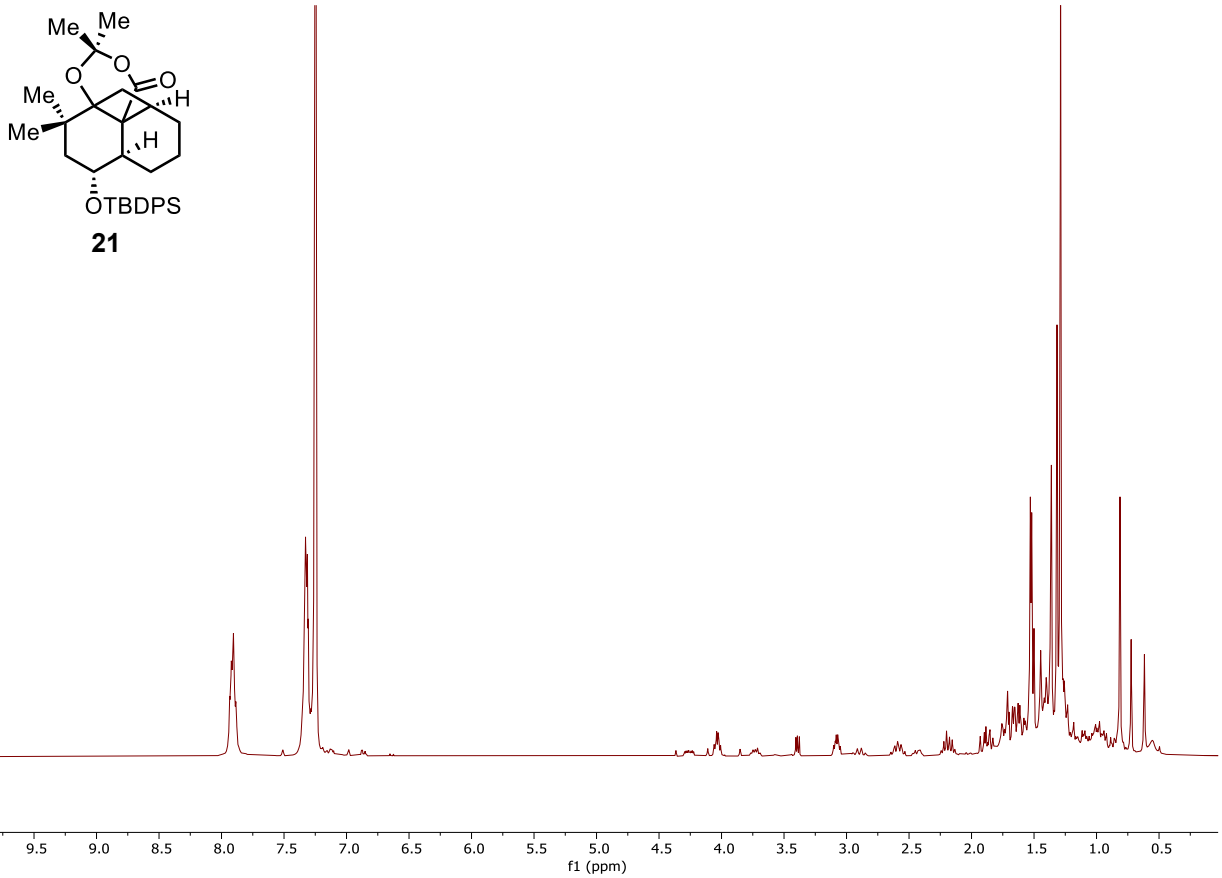
Me
Me
O
O
O
H
Me
Me
H
OTBDPS
21
9.5
9.0
8.5
8.0
7.5
7.0
6.5
6.0
5.5
5.0
4.5
4.0
3.5
3.0
2.5
2.0
1.5
1.0
0.5
f1 (ppm)

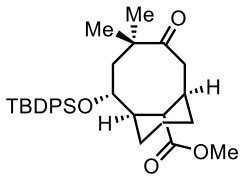
Me
O
Me
H
TBDPSO
H
OMe
O

23

9.5
9.0
8.5
8.0
7.5
7.0
6.5
6.0
5.5
5.0
4.5
4.0
3.5
3.0
2.5
2.0
1.5
1.0
0.5
0.0
f1 (ppm)

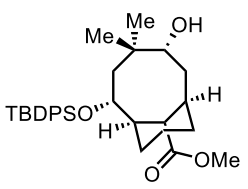
Me
OH
Me
H
TBDPSO
H
O
OMe

24

9.5
9.0
8.5
8.0
7.5
7.0
6.5
6.0
5.5
5.0
4.5
4.0
3.5
3.0
2.5
2.0
1.5
1.0
0.5
0.0
f1 (ppm)

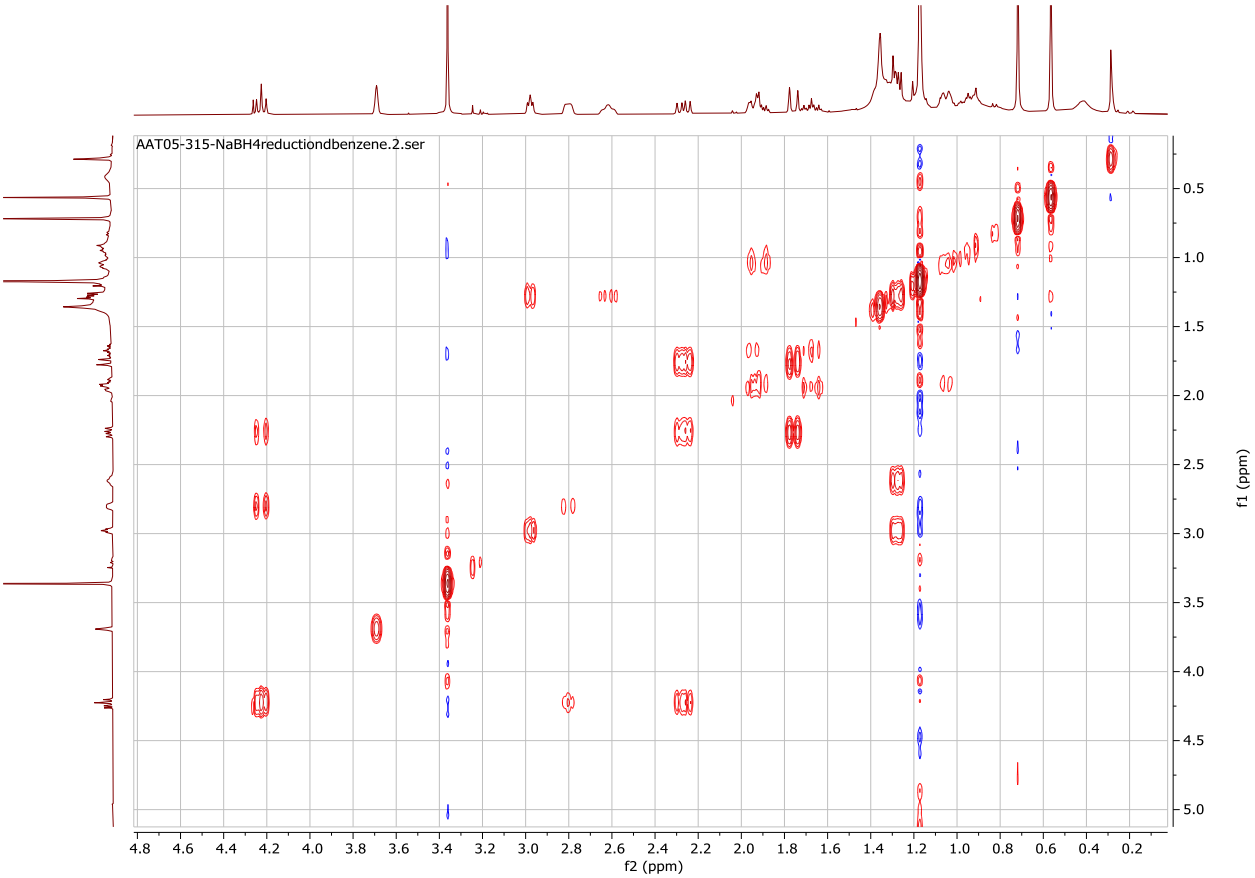
AAT05-315-NaBH4reductiondbenzene.2.ser
f2 (ppm)
f1 (ppm)

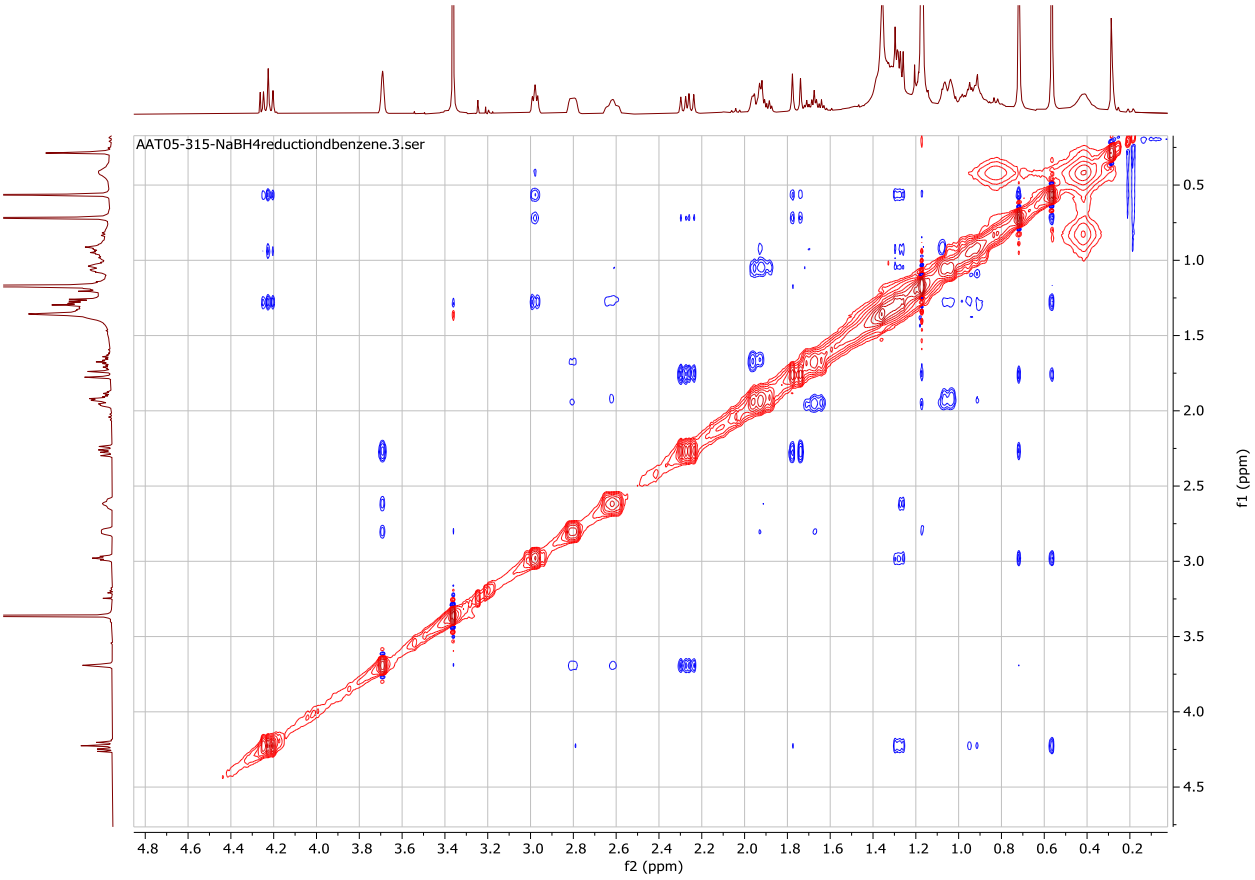
AAT05-315-NaBH4reductiondbenzene.3.ser
f2 (ppm)
f1 (ppm)

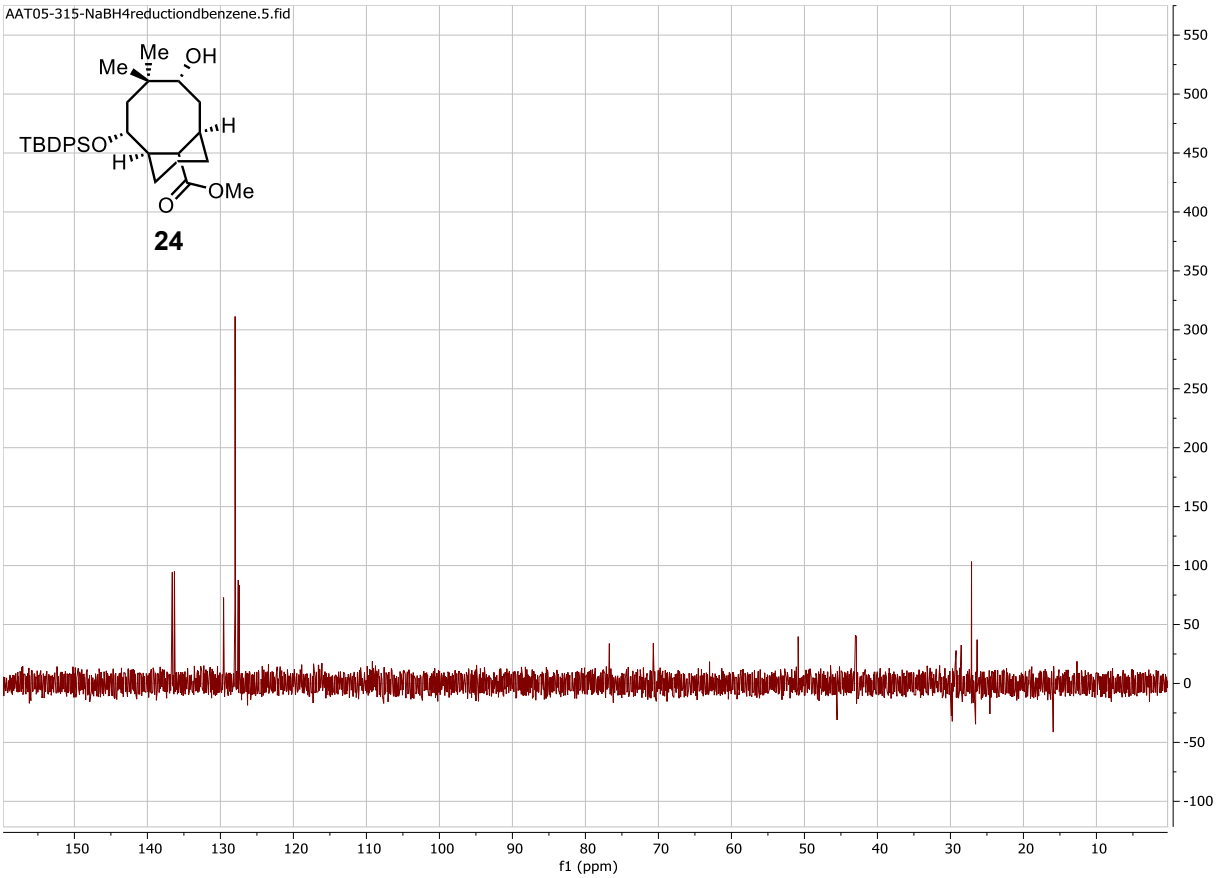
AAT05-315-NaBH4reductiondbenzene.5.fid
Me
OH
Me
H
TBDPSO
H
O
OMe
24
550
500
450
400
350
300
250
200
150
100
50
0
-50
-100
150
140
130
120
110
100
90
80
70
60
50
40
30
20
10
f1 (ppm)

Chapter 2

Development of ADC-TACs: Antibody-small molecule conjugates for targeted degradation of GPCRs

Abstract

Proteolysis Targeting Chimeras (PROTACs) have emerged as a groundbreaking advancement in chemical biology and therapeutic development, with at least 18 currently in phase I/II clinical trials. PROTACs are heterobifunctional molecules that facilitate protein degradation by recruiting an E3 ligase to the target protein of interest, resulting in ubiquitination and subsequent degradation. In recent years, novel methods for targeted degradation of membrane protein have also been developed such as AbTACs, which make use of a bispecific antibody scaffold to recruit membrane-bound E3 ligases to the target. However, multi-pass membrane proteins such as G protein-coupled receptors (GPCRs) remain difficult to degrade with such technology, as there are few extracellular-binding antibodies. In collaboration with the laboratory of James Wells, PhD., we are developing an alternative modality to expand the scope of AbTACs by conjugating an E3 ligase targeting antibody to a small molecule binder of a GPCR of interest, effectively repurposing antibody-drug conjugates (ADCs) for protein degradation. We hypothesize that these constructs will not only have the stability of an antibody, but also expand the range of possible membrane proteins for targeted degradation.

Introduction

Over the past two decades, targeted protein degradation (TPD) has emerged as a groundbreaking therapeutic strategy, offering an alternative to traditional small-molecule inhibitors. While small-molecule inhibitors typically operate through occupation of a binding site where high potency is required to temporarily inhibit protein activity, TPD leverages existing cell biology to catalytically degrade target proteins. This catalytic mechanism enables a single molecule to induce the degradation of multiple copies of the same target, enhancing therapeutic efficacy and reducing the required dose compared to conventional inhibitors.[49]

Proteolysis targeting chimeras (PROTACs) are heterobifunctional small molecules that recruit the E3 ubiquitin ligase to the target protein of interest (POI), facilitating ubiquitination and subsequent degradation by the proteasome. Due to this design, PROTACs are able to degrade proteins by binding any accessible epitope, rather than targeting an enzyme's active site as in traditional inhibitors.[50] PROTACs have shown significant promise, with several progressing to clinical trials.[51] While PROTACs have proven successful in targeting intracellular proteins, however, they are generally limited to this scope.

Novel methods have been developed specifically for the degradation of membrane-bound proteins, such as AbTACs, which utilizes a bispecific antibody scaffold to recruit a membrane-bound E3 ligase in proximity to another membrane-bound protein of interest.[52] Other strategies have also emerged utilizing internalizing receptors for lysosome-based degradation, such as KineTACs and LyTACs.[53,54] However, these technologies inherently depend on there being an antibody or

antibody-based fragment against the POI. Due to this limitation, the ability to degrade multi-pass membrane proteins, such as G-protein coupled receptors (GPCRs), remains a challenge. There are few extracellular-binding antibodies that exist for this class of proteins, which lack a large, structured ectodomain for antibody binding.[55]

In order to expand the scope of TPD to include such challenging targets, we are developing a novel modality that effectively expands upon AbTACs. While there may be a lack of antibodies against GPCRs, there is a wide breadth of known and well-validated small molecule binders. By using one of the small molecules as the POI targeting arm and chemically linking it to an existing antibody degrader (anti-RNF43), we can synthesize an antibody-drug conjugate PROTAC, termed ADC-TACs (**Figure 2.1**). Here, we describe the synthesis of ADC-TACs as well as preliminary data for the degradation of adenosine 2A receptor (A2AR).

Results

As a proof-of-concept, we sought to see if we could develop constructs for the degradation of the A2AR. A2AR is a GPCR expressed on immune cells like natural killer (NK) and CD8+ T cells, and is activated by elevated extracellular adenosine, triggering a signaling cascade that increases intracellular cAMP and induces immunosuppression. In the tumor microenvironment (TME), high ATP levels are converted to adenosine, enhancing A2AR activity.[56] Beyond immune suppression, A2AR activation promotes cancer cell proliferation via the MAPK/ERK/JNK pathways. This overactivity, driven by excess adenosine in the TME, both dampens immune responses and supports tumor growth.[57] As a result, A2AR antagonists are being explored as potential therapies

to block its immunosuppressive effects and inhibit cancer proliferation. With the aforementioned noted, A2AR appeared to be a desirable target for degradation and chosen as our POI for the development of ADC-TACs.

CGS21680 is a known small molecule agonist of A2AR that has been previously conjugated to the Fc domain of an antibody.[58] In a crystal structure of CGS21680 bound to A2AR, the carboxylic acid functionality of the molecule is solvent exposed, enabling it is a conjugation site that would not interfere with small molecule binding.[59] We synthesized analogs of CGS21680 containing a polyethylene glycol (PEG) linker (n= 4,6,9,12, and 23) and dibenzocylooctyne (DBCO) functional group through an amide bond formation (**Figure 2.2a**). In order to conjugate these molecules to anti-RNF43 E3 ligase fabs in a site-specific manner, we utilized methionine-specific oxaziridine chemistry with an oxaziridine-azide reagent (**Figure 2.2b**).[60] Methionine residues were introduced into sites in the fab scaffold that have been previously validated to show high labeling stability and efficiency.[61] The anti-RNF43 fab mutants were then labeled with oxaziridine reagent to functionally install an azide handle, which could then undergo copper-free click chemistry labeling upon incubation with DBCO-PEG-CGS21680 conjugates.

Our initial degradation experiments were performed in MOLT-4 cells, which endogenously express both A2AR and RNF43. Cells were dosed with varying concentrations of synthesized ADC-TAC, and degradation was assessed through Western blotting for A2AR levels. Unfortunately, even after testing constructs with 4 different sites of labeling and various PEG linker lengths, we were unable to see consistent A2AR degradation (**Figure 2.3**). We hypothesized

that a potential factor in limited degradation could be the inherently low expression levels of RNF43 in MOLT-4 cells. As we also found that it was difficult to identify another cell line that also co-expressed A2AR and RNF43, we chose alternative strategies for A2AR degradation.

First, we looked to using ZNRF3, an alternative cell surface E3 ligase that is co-expressed with A2AR in Jurkat cells.[63] We performed the same bioconjugation strategy with our DBCO-PEG-CGS21680 molecules with anti-ZNRF3 fabs in order to obtain a new library of constructs. However, we could still not see consistent levels of degradation in Jurkat cells.

Second, we are currently looking to adapt KineTACs into our ADC-TAC modality instead of using an antibody against a membrane-bound E3 ligase. One potential pitfall of E3 ligase recruitment is that there may be geometry requirements for the linker, POI, and E3 ligase in order for ubiquitination to successfully occur. KineTACs use a bispecific IgG scaffold where one arm targets a POI, and the other is recombinant chemokine CXCL12, a chemokine that targets a constitutively internalizing decoy receptor, CXCR7. We have conjugated DBCO-PEG-CGS21680 to methionine scrubbed CXCL12-Fc fusion with a V262M mutation. Degradation experiments will proceed in MDA-MB-361 cells, which express both A2AR and CXCR7.

Methods

Cell lines Cell lines were grown and maintained in T75 (Thermo Fisher Scientific) flasks at 37ºC and 5% CO2. MOLT-4 CCR5+ cells were grown in RPMI-1640 supplemented with 10% fetal bovine serum (FBS) and 2% geneticin. MOLT-4 CCR5+ cells were obtained from the NIH AIDS Reagent Program.

Antibody cloning, expression, and purification Anti-RNF43 Fab LC S7M single mutation was introduced using Gibson Assembly. Fabs were expressed in E. coli C43(DE3) Pro+ using an optimized autoinduction media and purified by Protein A affinity chromatography. Purity and integrity of Fabs were assessed by SDS-PAGE and intact LC/MS mass spectrometry (Waters).

Representative Synthesis of DBCO-CGS21680 (PEG 4 linker) To a 10 mL RBF charged with commercially available CGS21680 (Cayman Chemical, 17126, 2.0 mg, 4.0 μmol) was added 2 mL of dimethylformamide. 1-[Bis(dimethylamino)methylene]-1H-1,2,3-triazolo[4,5-b]pyridinium 3-oxide hexafluorophosphate (HATU) (2.3 mg, 1.5 eq, 6 μmol) and N,N-diisopropylethylamine (2.8 μL, 4.0 Eq, 16.0 μmol) were then added sequentially, and the reaction was allowed to stir at room temperature for 15 minutes. DBCO-PEG4-amine (BroadPharm, BP-23958, 3.1 mg, 1.5 Eq, 6.0 μmol) was then added, and the reaction mixture was allowed to stir for an additional 16 hours. The reaction mixture was then concentrated in vacuo, and the residue was purified by high performance liquid chromatography (HPLC) and lyophilized to afford DBCO-PEG4-CGS21680 (1.5 mg, 1.5 μmol, 37%) as a light yellow solid.

Conjugation of engineered anti-RNF43 Fab with oxaziridine and DBCO-CGS21680 75 For conjugation with oxaziridine, 50 μM Fab was incubated with 5 molar equivalents of oxaziridine azide for 30 min at room temperature in phosphate-buffer saline (PBS). The reaction was quenched with 10 molar equivalents methionine. The antibody was buffer exchanged into PBS and desalted using a 0.5-mL Zeba 7-kDa desalting column (Thermo Fisher Scientific). Then, 10 molar equivalents of DBCO-CGS21680 was added and incubated at room temperature overnight. The agonist-labeled conjugate was desalted using the 0.5-mL Zeba 7-kDa desalting column to remove excess DBCO-CGS21680. Full conjugation at each step was monitored by intact mass spectrometry using a Xevo G2-XS Mass Spectrometer (Waters).

Degradation assays Cells at 1 million cells/mL were treated with antibody-drug conjugate, agonist, or antagonist in complete growth medium. After 24 hrs, cells were pelleted by centrifugation (300xg, 5 min, 4ºC). Cell pellets were lysed with RIPA buffer containing cOmplete mini protease inhibitor cocktail on ice for 40 min. Lysates were spun at 16,000xg for 10 min at 4ºC and protein concentrations were normalized using BCA assay. 4x NuPAGE LDS sample buffer and 2-mercaptoethanol (BME) was added to the lysates. Equal amounts of lysates were loaded onto a 4-12% Bis-Tris gel and ran at 200V for 37 min. The gel was incubated in 20% ethanol for 10 min and then transferred onto a polyvinylidene difluoride (PVDF) membrane. The membrane was blocked in PBS with 0.1% Tween20 + 5% bovine serum albumin (BSA) for 30 min at room temperature with gentle shaking. Membranes were co-incubated overnight with rabbit-anti-A2aR (Abcam, ab3461, 1:1000) and mouse-anti-tubulin (Cell Signaling Technologies, DM1A, 1:1600) at 4ºC with gentle shaking in PBS + 0.2% Tween20 + 5% BSA. Membranes were washed four times with tris-buffered saline (TBS) + 0.1% Tween20 and then co-incubated with HRP-anti-rabbit

IgG (Cell Signaling Technologies, 7074S, 1:2000) and 680RD goat anti-mouse IgG (LI-COR, 926-68070, 1:10000) in PBS + 0.2% Tween20 + 5% BSA for 1 hr at room temperature. Membranes were washed four times with TBS + 0.1% Tween20, then washed with PBS. Membranes were first imaged using an 76 OdysseyCLxImager (LI-COR). SuperSignal West Pico PLUS Chemiluminescent Substrate was then added and image using a ChemiDoc Imager (BioRad). Band intensities were quantified using Image Studio Software (LI-COR).

Figures

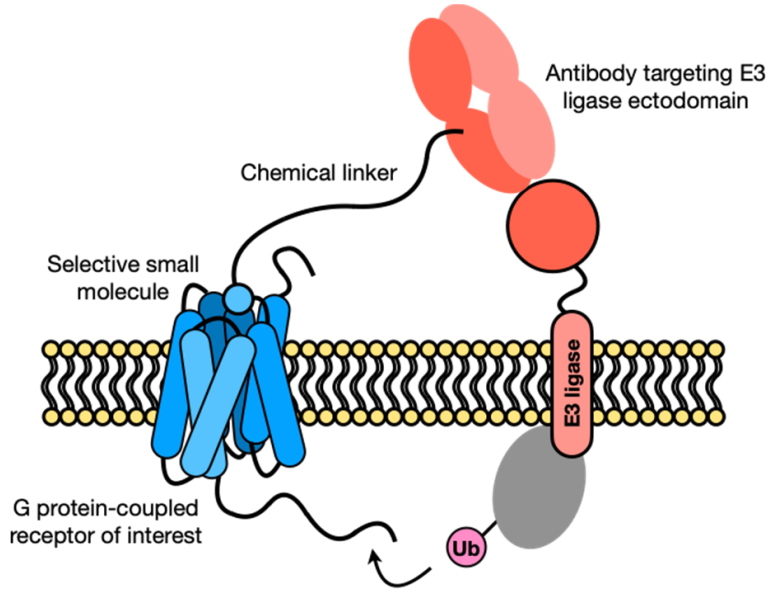

Figure 2.1: Mechanism of action of ADC-TACs in the targeted degradation of cell surface proteins. Degradation is induced using an ADC-TAC to recruit an E3 ligase to a cell surface protein of interest. A selective small molecule is used for binding to the protein of interest and is chemically linked to an antibody targeting the E3 ligase.

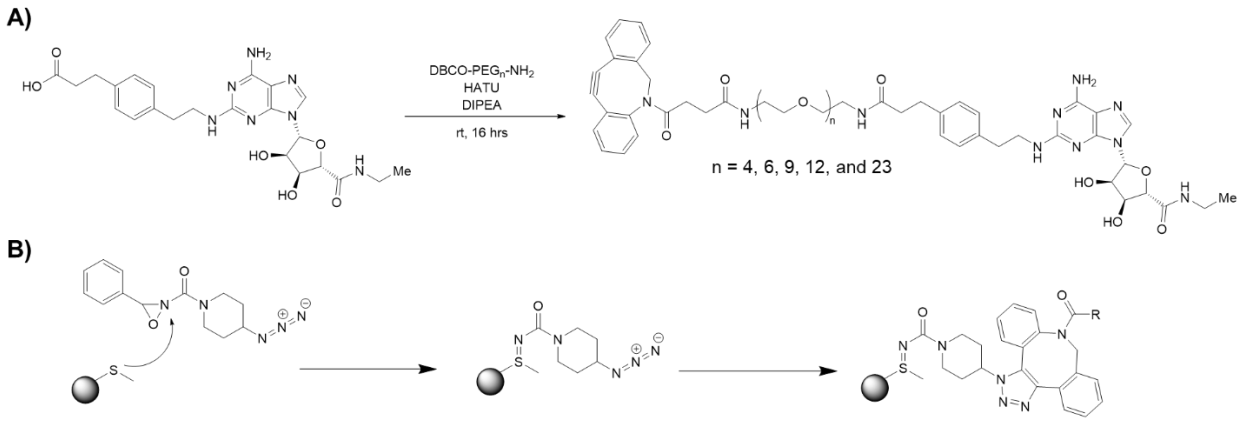

Figure 2.2: **Bioconjugation strategy for ADC-TACs. A.** Synthesis of DBCO-PEG$_n$-CGS21680 through amide coupling. **B.** Methionine-oxaziridine labeling, followed by copper-free click chemistry labeling.

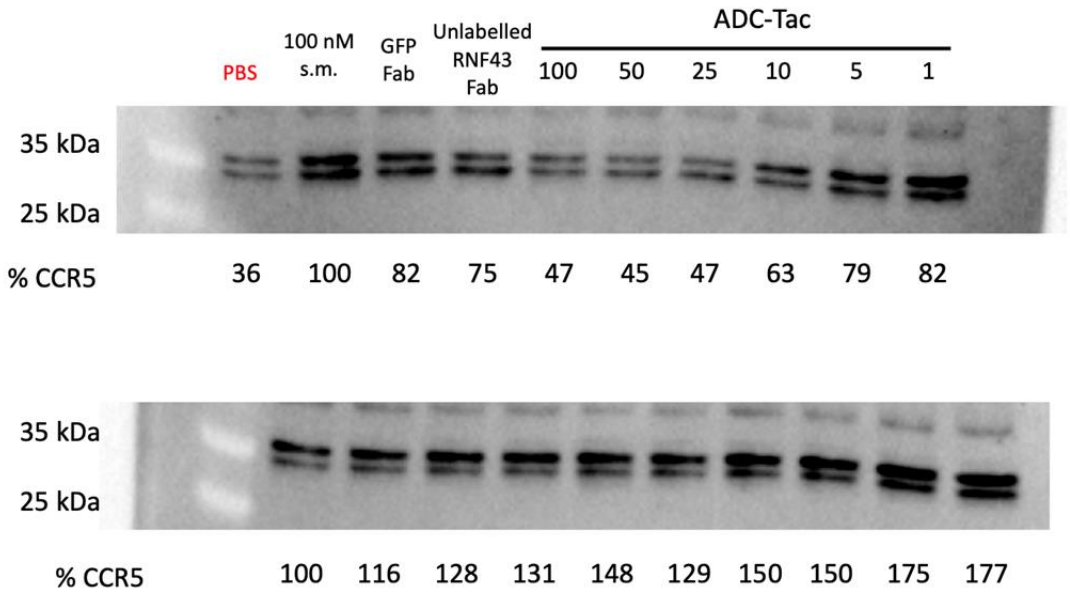

Figure 2.3: **Representative Western blots for A2AR degradation**. Biological duplicates show inconsistency in degradation of A2AR in MOLT-4 cells. The top blot shows what appears to be dose-dependent degradation of A2AR from 100 nM down to 1 nM of ADC-TAC, where as the bottom blot shows no degradation of A2AR.

References

1. Wright, P. M.; Seiple, I. B.; Myers, A. G. The Evolving Role of Chemical Synthesis in Antibacterial Drug Discovery. *Angew. Chem. Int. Ed.* **2014**, *53*, 8840-8869.
2. Silver, L. L. Challenges of Antibacterial Discovery. *Clin. Microbiol. Rev.* **2011**, *24*, 71–109.
3. Walsh, C. Where will new antibiotics come from? *Nature Rev. Microbiol*. **2003,** *1*, 65-70.
4. Poehlsgaard, J.; Douthwaite, S. The bacterial ribosome as a target for antibiotics. *Nature Rev. Microbiol.* **2005**, *3,* 870-881.
5. Wilson, D.N. Ribsosome-targeting antibiotics and mechanisms of bacterial resistance. *Nature Rev. Microbiol.* **2014**, *12*, 35-48.
6. Paukner, S.; Riedl, R. Pleuromutilins: Potent Drugs for Resistant Bugs – Mode of Action and Resistance. *Cold Spring Harb Perspect Med.* **2017**, *7*:a027110.
7. Kavanagh, F.; Hervey, A.; Robbins, W. J. Antibiotic substances from basidiomycetes: viii. pleurotus mutilus (Fr.) Sacc. And pleurotus passeckerinaus pilat. *Proc. Nat. Acad. Sci.* **1951**, *37*, 570-574.
8. Anchel, M. Chemical studies with pleuromutilin. *J. Biol. Chem.* **1952**, *199*, 133-139.
9. Szybalski, W. Genetic studies on microbial cross resistance to toxic agents. IV. Cross resistance of Bacillus megaterium to forty-four antimicrobial drugs. *Appl. Microbiol*. **1954**, *2*, 57-63.
10. Knauseder, F.; Brandl, E. Pleuromutilins. Fermentation, structure, and biosynthesis. *J. Antibiot*. (*Tokyo*). **1976**, *29*, 125-131.
11. Novak, R. Are pleuromutilin antibiotics finally fit for human use? *Ann. N. Y. Acad. Sci.* **2011**, *1241*, 71-81.

12. Drews, J.; Georgopoulos, A.; Laber, G.; Schütze,E.; Unger, J. Antimicrobial activities of 81.723 hfu, a new pleuromutilin derivative. *Antimicrob. Agents Chemother.* **1975**, *7*, 507-516.

13. Burch, D. G. S.; Ripley, P. H.; Zeisl, E. Patent WO1998001127 A1, **1998**.

14. Heilmann, C.; Jensen, L.; Jensen, J. S.; Lundstrom, K.; Windsor, D.; Windsor, H.; Webster, D. Treatment of resistant mycoplasma infection in immunocompromised patients with a new pleuromutilin antibiotic. *J. Infect.* **2001**, *43*, 234-238.

15. Jacobs, M. R. Retapamulin: a semisynthetic pleuromutilin compound for topical treatment of skin infections in adults and children. *Future Microbiol.* **2007**, *2*, 591-600.

16. Sun, F.; Zhang, H.; Gonzales, G. B.; Zhou, J; Li, Y.; Zhang, J.; Jin, Y.; Wang, Z.; Li, Y.; Cao, X.; Zhang, S.; Yang, S. Unraveling the Metabolic Route of Retapamulin: Insights into Drug Development of Pleuromutilins. *Antimicrob. Agents Chemother.* **2018**, *62*:e02388-17.

17. Springer, D. M.; Sorenson, M. E.; Huang, S.; Connolly, T. P.; Bronson, J. J.; Matson, J. A.; Hanson, R. L.; Brzozowski, D. B.; LaPorte, T. L.; Patel, R. N. Synthesis and activity of a C-8 keto pleuromutilin derivative. *Bioorg Med Chem Lett*. **2003**, *13*, 1751-1753

18. Mang, R.; Heilmayer, W.; Badegruber, R.; Strickmann, D.; Novak, R.; Ferencic, M.; Bulusu, A. R. C. M. Pleuromutilin derivatives for the treatment of diseases mediated by microbes. Patent WO2008113089, **2008**.

19. Goethe, O.; Heuer, A.; Ma, X.; Wang, Z.; Herzon, S. B. Antibacterial properities and clinical potential of pleuromutilins. *Nat. Prod. Rep.* **2019**, *36*, 220-247.

20. Andemichael, Y. W.; Chen, J.; Clawson, J.S.; Dai, W.; Diederich, A.; Downing, S.V.; Freyer, A.J.; Liu, P.; Oh, L. M.; Patience, D. B.; Sharpe, S.; Sisko, J.; Tsui, J.; Vogt, F. G.;

Wang, J.; Wernersbach, L.; Webb, E. C.; Wertman, J.; Zhou, L. Process development for a novel pleuromutilin-derived antibiotic. *Org Process Res Dev*. **2009**, *13*, 729-738.

21. Novak, R.; Shlaes, D. M. The pleuromutilin antibiotics: a new class for human use. *Curr. Opin. Investig. Drugs.* **2010**, *11*, 182-191.
22. Hunt, E. Pleuomutilin antibiotics. *Drugs Future.* **2009**, *25*, 1163-1168.
23. Gibbons, E. G. Total synthesis of (±)-pleuromutilin. *J. Am. Chem. Soc.* **1982**, *104*, 1767-1769.
24. Boeckman, R. K.; Springer, D. M.; Alessi, T. R. Synthetic studies directed toward naturally occurring cyclooctanoids. 2. A stereocontrolled assembly of (±)-pleuromutilin via a remarkable sterically demanding oxy-Cope rearrangement. *J. Am. Chem. Soc.* **1989**, *111*, 8284-8286.
25. Fazakerley, N. J.; Helm, M. D.; Procter, D. J. Total synthesis of (+)-pleuromutilin. *Chem.-Eur. J.* **2013**, *19*, 6718-6723.
26. Murphy, S. K.; Zeng, M; Herzon, S. B. A modular and enantioselective synthesis of the pleuromutilin antibiotics. *Science*. **2017**, *356*, 956-959.
27. Zeng, M.; Murphy, S. K.; Herzon, S. B. Development of a Modular Synthetic Route to (+)-Pleuromutilin, (+)-12-*epi*-Mutilins, and Related Structures. *J. Am. Chem. Soc.* **2017**, *139*, 16377-16388.
28. Farney, E. P.; Feng, S. S.; Schäfers, F.; Reisman, S. E. Total Synthesis of (+)-Pleuromutilin *J. Am. Chem. Soc.* **2018**, *140*, 1267-1270.
29. Foy, N. J.; Pronin, S. V. Synthesis of Pleuromutilin. *J. Am. Chem. Soc.* **2022**, *144*, 10174-10179.

30. Chen, H.; Li, Z.; Shao, P.; Yuan, H.; Chen, S.; Luo, T. Total Synthesis of (+)-Mutilin *J. Am. Chem. Soc.* **2022**, *144*, 15462-15467.

31. Goethe, O.; DiBello, M.; Herzon, S. B. Total synthesis of strrructrually diverse pleuromutilin antibiotics. *Nat. Chem.* **2022**, *14*, 1270-1277.

32. Berner, H.; Vyplel, H.; Schulz, G.; Scheider, H. Chemie der Pleuromutiline, 11. Mitt.: Konfigurationsumkehr der Vinylgruppe am Kohlenstoff 12 durch reversible Retro-En-Spaltung. *Monatsh. Chem.* **1986**, *117*, 1073-1080.

33. Thirring, K.; Heilmayer, W.; Riedl, R.; Kollmann, H.; Ivezic-Schoenfeld, Z.; Wicha, W.; Paukner, S.; Strickmann, D. Patent WO2015110481, **2015**.

34. Paukner, S.; Wicha, W. W.; Heilmayer, W.; Thirring, K.; Riedl, R, presented in part at the *Interscience Conference of Antimicrobial Agents and Chemotherapy/International Congress of Chemotherapy and Infection (ICAAC/ICC)*, San Diego, CA, **2015**.

35. Liu, J.; Lotesta, S. D.; Sorensen, E. J. A concise synthesis of the molecular framework of pleuromutilin. *Chem. Commun.* **2011**, *47*, 1500-1502.

36. Lotesta, S. D.; Liu, J.; Yates, E. V.; Krieger, I.; Sacchettini, J. C.; Freundlich, J. S.; Sorensen, E. J. Expanding the pleuromutilin class of antibiotics by *de novo* chemical synthesis. **2011**, *2*, 1258-1261.

37. Springer, D. M.; Bunker, A.; Luh, B.; Sorenson, M. E.; Goodrich, J. T.; Bronson, J. J.; DenBleyker, K.; Dougherty, T. J.; Fung-Tomc, J. Cyclopentanone ring-cleaved pleuromutilin derivatives. *Eur. J. Med. Chem.* **2007**, *42*, 109-113.

38. Nagaoka, H.; Ohsawa, K.; Takata, T.; Yamada, Y. A new synthetic approach to the bicyclo[5,3,1]undecane ring system in taxanes. *Tetrahedron Lett.* **1984**, *25*, 5389-5392.

39. Mehta, G.; Reddy, K. S. A Facile Oxy-Cope Rearrangement Route to Functionalized Bicyclo[5,3,1]undecane Ring System Present in Taxol and Vinigrol Diterpenoids. *Synlett*. **1996**, *7*, 625-627

40. Snider, B. B.; Allentoff, A. J. Synthesis of the Bicyclo[5,3,1]undecane Moiety (AB Ring System) of Taxanes. *J. Org. Chem.* **1990**, *56*, 321-328.

41. De Mayo, P.; Takashita, H.; Satter, A. B. M. A. The Photochemical Synthesis of 1,5-Diketones and their Cyclisation. A new Annulation Process. *Proc. Chem. Soc.* **1962**, 119.

42. Winkler, J. D.; Hey, J. P. Inside-Outside Stereoisomerism: The Synthesis of *tran*-Bicyclo[5,3,1]undecan-11-one. *J. Am. Chem. Soc.* **1986**, *108*, 6425-6427.

43. Winkler, J. D.; Muller, C. L.; Hey, J. P.; Ogilvie, R. J.; Haddad, N. The effect of chromophore transposition on the stereochemical outcome of the intramolecular dioxenone photocycloaddition reaction. *Tetrahedron Lett.* **1989**, *30*, 5211-5214.

44. Mander, L. N.; Sethi, S. P. Regioselective synthesis of -*β*-ketoesters from lithium enolates and methyl cyanoformate. *Tetrahedron Lett.* **1983**, *24*, 5425-5428.

45. Kim, D.; Lim, H. N. An expedient synthesis of cyanoformates *via* DAST-mediated C-C bond cleavage of *α*-oximino-*β*-ketoesters. *Tetrahedron Lett.* **2021**, *73*, 153116.

46. Winkler, J. D.; Subrahmanyam, D. Studies Directed Towards the Synthesis of Taxol: Preparation of C-13 Oxygenated Taxane Congeners. *Tetrahedron*. **1992**, *48*, 7049-7056.

47. Paulisch, T. O.; Mai, L. A.; Strieth-Kalthoff, F; James, M. J.; Henkel, C.; Guldi, D. M.; Glorius, F. Dynamic Kinetic Senstitization of *β*-Dicarbonyl Compounds – Access to Medium-Sized Rings by De Mayo-Type Ring Expansion. *Angew. Chem. Int. Ed.* **2022**, *61*, e202112695.

48. Winkler, J. D.; Henegar, K. E.; Hong, B.; Williard, P. G. Inside-outside stereoisomerism. 6. Synthesis of *tran*-Bicyclo[4,4,1]undecan-11-one and the First Stereoselective Construction of the Tricyclic Nucleus of the Ring system of Ingenane Diterpenes. *J. Am. Chem. Soc.* **1994**, *116*, 4183-4188.

49. Zhao, L.; Khao, J.; Zhong, K.; Tong, A.; Jia, D. Targeted protein degradation: mechanisms, strategies and application. *Sig. Transduct. Target. Ther.* **2022**, *7*, 113.

50. Pattersson, M.; Crew, C. M. PROteolysis Targeting Chimeras (PROTACs) – Past, present and future. *Drug. Discov. Today. Technol.* **2019**, *31*, 15-27.

51. Chirnomas, D.; Hornbergerr, K. R.; Crews, C. M. Protein degraders enter the clinic – a new approach to cancer therapy. *Nat. Rew. Clin. Oncol.* **2023**, *20*, 265-278.

52. Cotton, A. D.; Nguyen, D. P.; Gramespacher, J. A.; Seiple, I. B.; Wells, J. A. Development of Antibody-based PROTACs for the Degradation of the Cell-Surface Immune Checkpoint Protein PD-L1. *J. Am. Chem. Soc.* **2021**. *143*, 593-598.

53. Pance, K.; Gramespacher, J. A.; Byrnes, J. R.; Salangsang, F.; Serrano, J. C.; Cotton, A.D.; Steri, V.; Wells, J. A. Modular cytokine receptor-targeting chimerras for targeted degradation of cell surface and extracellular proteins. *Nat. Biotechnol.* **2023**, *41*, 273-281.

54. Banik, S. M.; Pedram, K.; Wisnovsky, S.; Ahn, G.; Riley, N. M.; Bertozzi, C. R. Lysosome-targeting chimeras for degradation of extracellular proteins. *Nature*. **2020**, *584*, 291-297.

55. Schlimgen, R. R.; Peterson, F. C.; Heukers, R.; Smit, M. J.; McCorvy, J. D.; Volkman, B. F. Structural basis of selectivity and antagonism in extracellular GPCR-nanobodies. *Nat. Commun.* **2024**, *15*, 4611.

56. Vijayan, D; Young, A.; Teng, M. W. L.; Smyth, M. J. Targeting immunosuppressive adenosine in cancer. *Nat. Rev. Cancer.* **2017**, *17*, 709-724.

57. Sek, K.; Mølck, C.; Stewart, G. D.; Kats, L.; Darcy, P. K.; Beavis, P. A. Targeting Adenosine Receptor Signaling in Cancer Immunotherapy. *Int. J. Mol. Sci.* **2018**, *19*, 3837.

58. Chiang, M.; Holbert, M. A.; Halin, J. H.; Ahn, Y.; Giddens, J.; Amin, M. N.; Taylor, M. S.; Collins, S. L.; Chan-Li, Y.; Waickman, A.; Hsiao, P.; Bolduc, D.; Leahy, D. J.; Horton, M. R.; Wang, L.; Powell, J. D.; Cole, P. A. An Fc Domain Protein-Small Molecule Conjugate as an Enhanced Immunomodulator. *J. Am. Chem. Soc.* **2014**, *136*, 3370-3373.

59. Lebon, G.; Edwards, P. C.; Leslie, A. G. W.; Tate, C. G. Molecular Determinants of CGS21680 Binding to the Human Adenosine A2A Receptor. *Mol. Pharmacol.* **2015**, *87*, 907-915.

60. Lin, S.; Yang, X.; Jia, S.; Weeks, A. M.; Hornsby, M.; Lee, P. S.; Nichiporuk, R. V.; Iavarone, A. T.; Wells, J. A.; Toste, F. D.; Chang, C. J. Redox-based reagents for chemoselective methionine bioconjugation. *Science*. **2017**, *355*, 597-602.

61. Elledge, S. K.; Tran, H. L.; Christian, A. H.; Steri, V.; Hann, B.; Toste, F. D., Chang, C. J.; Wells, J. A. Systematic identification of engineered methionines and oxaziridines for efficient, stable, and site-specific antibody bioconjugation. **2020**, *117*, 5733-5740.

62. Gramespacher, J. A.; Cotton, A. D.; Burroughs, P. W. W.; Seiple, I. B.; Wells, J. A. Roadmap for Optimizing and Broadening Antibody-Based PROTACs for Degradation of Cell Surface Proteins. **2022**, *17*, 1259-1268.

Publishing Agreement

It is the policy of the University to encourage open access and broad distribution of all theses, dissertations, and manuscripts. The Graduate Division will facilitate the distribution of UCSF theses, dissertations, and manuscripts to the UCSF Library for open access and distribution. UCSF will make such theses, dissertations, and manuscripts accessible to the public and will take reasonable steps to preserve these works in perpetuity.

I hereby grant the non-exclusive, perpetual right to The Regents of the University of California to reproduce, publicly display, distribute, preserve, and publish copies of my thesis, dissertation, or manuscript in any form or media, now existing or later derived, including access online for teaching, research, and public service purposes.

DocuSigned by:
Arthur Tran
3D0D1BB96FD749B...
Author Signature

12/11/2024
Date